

California State University, Northridge

Determination of the Geometry for a Ram-Air Parachute Canopy
in Steady Flight Through Numerical Simulations

A thesis submitted in partial fulfillment of the requirements
For the degree of Master of Science in
Mechanical Engineering

By

Robert Jonathan Fernandez Peralta

May 2015

The Master's thesis of Robert Jonathan Fernandez Peralta is approved:

Vibha Durgesh, Ph. D.

Date

George Youssef, Ph.D.

Date

Hamid Johari, Ph. D., Chair

Date

California State University, Northridge

Acknowledgments

This work has been supported by the U.S. Army Natick Soldier Research, Development and Engineering Center (NSRDEC). Results from this work has been presented at the 23rd American Institute of Aeronautics and Astronautics (AIAA) Decelerator Systems Technology Conference and Seminar, April 2015.

First I would like to thank my thesis advisor Dr. Hamid Johari for his guidance throughout the length of this project. His knowledge and experience in the subject of parachutes and parachute design has been truly inspiring and a great aid in accomplishing the goals of this project. I would also like to thank my committee, Dr. Youssef and Dr. Durgesh, for the support and encouragement through the final stretch.

Thank you to Greg Noetscher as well as Dr. Ken Desabrais and Dr. Keith Burgeron from NSRDEC for positively reinforcing the results in this paper and helping me gain access to the HPC resources. Thanks to Ben Tutt from Airborne Systems and Chinh Nguyen from Altair for assisting me in developing the necessary skills to effectively maneuver through LS-DYNA and HyperMesh software suites.

Lastly, I would like to extend my deepest gratitude to my friends and family for their understanding and continuing support through everything I have done and plan to do. Thank you for helping me keep everything in perspective.

Dedication

A special dedication for this thesis goes to my parents, Roy and Bess. You two have been the most encouraging and caring parents anyone can ask for. From something as simple as coffee to giving me my space when I need it, I really appreciate it. Your "work hard but enjoy life" personalities have played a large role in Ate Celeste's and my life. Being a fraction of the role models you two are would honestly make a better person than many of whom I've met. Thank you and I love you guys.

Table of Contents

Signature Page.....	ii
Acknowledgments.....	iii
Dedication.....	iv
List of Figures.....	vii
List of Tables.....	ix
Abstract.....	x
1. Introduction.....	1
1.1 Finite Element Method (FEM).....	4
1.2 Literature Review.....	5
1.3 Goals.....	7
2. Model Development.....	9
2.1 Model Setup.....	9
2.1.1 Solid Model.....	10
2.1.2 Surface Membrane.....	11
2.1.3 Element Membrane.....	13
2.2 Model Properties.....	14
2.2.1 Material Properties.....	14
2.2.2 Applied Loads.....	16
2.2.3 Constraints.....	17
3. Simulation.....	18
3.1 Technique Development.....	18
3.2 LS-DYNA Control Cards.....	21

4.	Canopy Parameters.....	22
	4.1 Defined Measurements.....	23
	4.2 Steady State Time.....	26
	4.3 Mesh Convergence.....	29
5.	Results.....	34
	5.1 Applied Pressure.....	34
	5.1.1 Uniformly Applied Pressure.....	35
	5.1.2 Variable Pressure in the Chordwise Direction (VPC).....	37
	5.1.3 Variable Pressure in the Chordwise and Spanwise Direction (VPCS)	39
	5.2 Implementing Control Lines.....	41
	5.2.1 Trailing Edge Measurements.....	41
	5.2.2 Control Lines.....	43
	5.3 Suspension Line Linear Density.....	44
	5.4 Vented Models.....	49
6.	Conclusion.....	51
	References.....	53
	Appendix A.....	55
	Appendix B.....	59
	Appendix C.....	60

List of Figures

Figure 1.1. MC-4 ram-air canopy anatomy.....	2
Figure 2.1. Solid model imported from SolidWorks to HyperMesh.....	10
Figure 2.2. Topology of canopy model.....	13
Figure 2.3. Undeformed ram-air canopy with 33037 elements in HyperMesh.....	14
Figure 3.1. Sequence of inflation.....	20
Figure 3.2. Zoomed in view of plot for applied pressure and applied suspension end node motion with time.....	21
Figure 4.1. Flow chart of steady state and mesh convergence study.....	23
Figure 4.2. Defined measurements.....	24
Figure 4.3. In-flight processed image; scale = 4.9.....	26
Figure 4.4. Image of N37615 (LE), N37575 (MCE) and N37542 (TE)	27
Figure 4.5. Steady state plot of displacement versus time for the chosen edge nodes taken from HyperGraph.....	28
Figure 4.6. Normalized displacement in time for leading edge node.....	28
Figure 4.7. Convergence of M5 at the 33k model.....	31
Figure 4.8. Variation of measurements with the number of elements.....	32
Figure 5.1. Variation of the 5 measurements with the applied pressures.....	37
Figure 5.2. Plot of net pressure for the middle half cell extracted from CFD data.....	38
Figure 5.3. Applied net pressure for VPC.....	39
Figure 5.4. Applied net pressure for VPCS.....	40
Figure 5.5. Steady state canopy for uniform applied pressures.....	41
Figure 5.6. Image of 3 measured nodes at the trailing edge of the canopy.....	42

Figure 5.7. Plot of trailing edge nodes with the applied pressure.....	43
Figure 5.8. Image of added control lines at 80% full extension.....	44
Figure 5.9. Unstable parachute system.....	45
Figure 5.10. Inflation after applying fixed nodes to the top leading edge of the canopy.....	45
Figure 5.11. Plot of suspension linear densities for M5.....	47
Figure 5.12. Suspension line linear density as a function of steady state time.....	48
Figure 5.13 Vented cases.....	49

List of Tables

Table 2.1. Ram-air parachute model properties.....	15
Table 4.1. Number of elements for each component of the ram-air canopy model.....	30
Table 4.2. Defined measurements for net pressure amplitude and distribution cases; 33k at t = 25 s.....	31
Table 5.1. Measurements taken for uniform pressure and variable pressure cases with the 33k model at t=25s.....	35
Table 5.2. Linear density and steady state time relationship.....	48

Abstract

Determination of the Geometry for a Ram-Air Parachute Canopy in Steady Flight Through Numerical Simulations

By

Robert Jonathan Fernandez Peralta

Master of Science in Mechanical Engineering

This paper discusses the application of Finite Element-based simulations to examine the geometry of a fully inflated, MC-4 ram-air parachute canopy in steady flight using a prescribed pressure distribution. Time and cost is always a factor in any engineering design, and until recently much of the design for parachute systems involved costly physical testing. Although these physical tests are very effective, Finite Element Methods provide an alternative to obtaining fairly accurate results at a fraction of the time and cost. Computer simulated systems are constantly proving their worth, and refining the strategies and techniques can only propel them forward in terms of reliability, accuracy and ease of use.

A novel approach for the inflation of the canopy from its cut-pattern was devised and implemented in LS-DYNA software suite. The effects of net pressure, pressure distribution, and material properties were explored by assessing various measures of the canopy geometry. Five specific measures considered were: maximum spanwise extent of

the canopy, radius of a circular arc fitted to the upper leading edge of the canopy, radius of individual half-cell openings, distance from the top of the canopy to the slider, and the maximum vertical distance between the canopy center and tip at the leading edge. A set of mesh refinement runs provided guidelines for acceptable average element area of 4.33 in²/element. These same runs aided in defining the time taken to reach a steady state. Variation of net applied pressure over a broad range resulted in minimal, less than 5%, change in the specific measures of the canopy geometry. This shows that the indicated technique can be used to reduce the use of resources to reach the resulting geometry of a fully inflated, steady state, canopy. This technique can be used in industry for preliminary design purposes in situations where a modification in the canopy is considered. It will give a good estimate to whether or not a modification will change the final, steady state, structure of the parachute system.

1. Introduction

History shows that the practice of parachute design has not changed significantly throughout the years. It was not until recently, in 1966, that Domina Jalbert [1] introduced the combination of a lift and drag type parachute. From Leonardo da Vinci's drag-based parachute sketch in the late 1400's to the current MC-4 military personnel canopy, it is clear that the main force components for flight are lift and drag. Although the design methodology has not changed, the development of new and improved parachutes have never been more prevalent. Modifications are constantly being made to improve the landing accuracy, durability, reliability and controllability of the parachute.

The modern day parachute systems cover a wide range of applications including deploying military personnel, delivering food and supplies, payload recovery, sport jumping and even resistance training. For this research paper, the parachute discussed will be the ram-air type parachute used for space and military functions.

Two forms of parachutes exist and are chosen depending on the goals of the user. The round type parachute uses drag as its main element to decelerate the payload. Current modifications involve changing the shape [2], from round to square, or adding vents to this drag-type system. Although these types of parachutes are still widely used today, the drag-based parachute has limitations in landing speed, landing accuracy and maneuverability. In order to accurately place a payload onto its target, the aircraft must deploy it at a low altitude. If the target is located in a hostile area, the low flying aircraft would be susceptible to attacks. To eliminate this risk, the aircraft must deploy the payload at a higher altitude, but with the variation in winds speeds and average maneuverability, the drop point becomes more difficult to hit [3]. For these reasons,

attention has been shifted to the research in improving the lift and drag based parachute, the parafoil or ram-air type parachute [4] shown in Fig. 1.1.

This parachute canopy consists of ribs sewn chordwise between the upper and lower membrane surfaces creating a series of cells. Each rib has a set of port holes to allow air to flow freely between the cells and consequently equalize pressure within the entire canopy. The leading edge of the canopy is open so that the ram air pressure maintains its airfoil shape. Suspension lines are typically attached to alternate ribs, or the edges of each full cell, to maintain the chordwise profile of the lower membrane surface. These lines are often cascaded to reduce drag. The slider is used to mitigate the shock created from the rapid inflation of the canopy as well as reducing tangling in the lines. The motion of the slider begins near the canopy and slides down the lines as the system deploys.

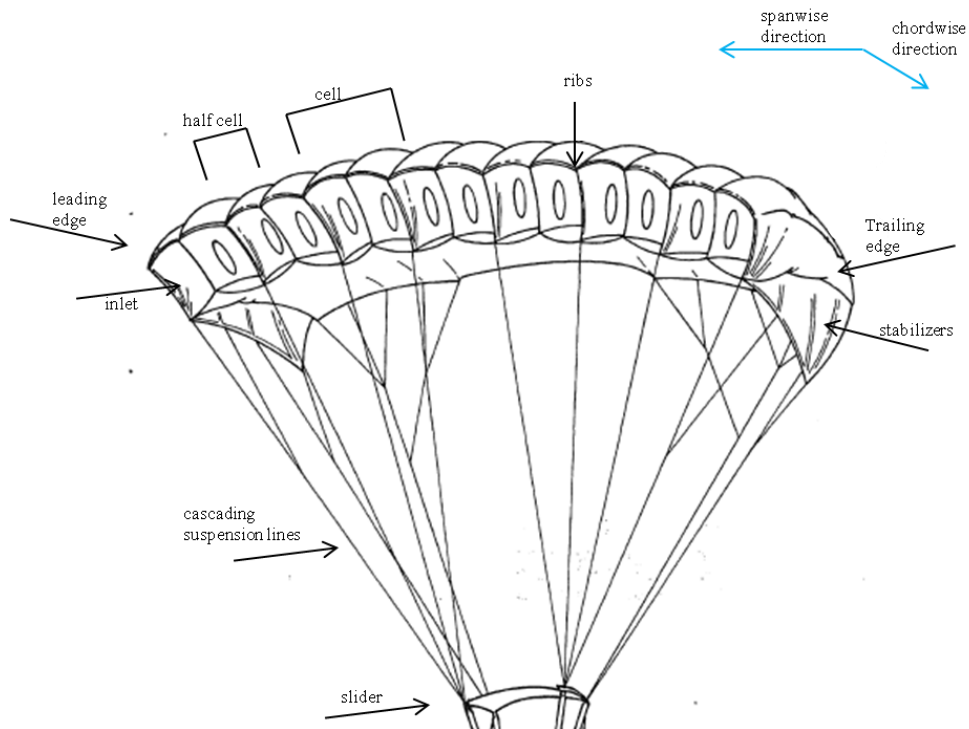


Figure 1.1. MC-4 ram-air canopy anatomy [4]

It is beneficial to use a ram-air canopy in applications that require soft landing, accurate landing and long range deployment. Through the combination of both lift and drag, the ram-air parachute excels in these applications. The MC-4 ram-air parachute has the ability to land at a velocity of 0-4 ft/s when deployed from an altitude of 25,000 feet. When a flared landing maneuver is used, the parachute can be placed within a few feet of its target [5].

Once the parachute is inflated and in flight, the ram-air canopy takes the form of a low aspect wing with an arc-anhedral curvature. This curvature is associated with the designed suspension line length. It plays an integral part in the gliding characteristics of the canopy. The lift to drag ratio, L/D , is another important characteristic of the ram-air canopy that can be improved by either increasing lift or decreasing drag. Lingard [3] states that there are many improvements that can be made with the ram-air parachutes including reducing drag at the inlet of the canopy or by modifying the arc-anhedral curvature of the wing. Making small modifications to the geometry of the canopy can play a large role in improving the performance of the system. One example of modifying the geometry would be to increase the spanwise length of the canopy giving the parachute system a larger aspect ratio and consequently more lift [3].

These modifications are typically done through physical drop tests and wind tunnel testing. Since multiple iterations must be made through the testing process, it can become very costly and take a lot of time to gather data and process it for results. Ever since the development of numerical simulation methods and high performance computers, there has been a demand to explore these capabilities and develop techniques

to simulate static and dynamic response of parachutes. In this project, the ram-air canopy in steady flight is considered.

1.1 Finite Element Method (FEM)

The development of finite element methods began in the 1940s for the field of structural engineering by Alexander Hrennikoff [6], and was further explored through the 1950s. Although numerical methods for solving engineering problems showed a lot of promise, the equations were too cumbersome to solve by hand making this method an improbable alternative to physical testing. It was not until the introduction of the high-speed digital computer in the late 1960s that finite element methods became an advantageous tool to solving engineering and multiphysics problems.

The theory behind finite element modeling (FEM) is to break down complicated problems into several smaller but simpler problems. FEM uses mathematical solutions and applies it to solid mechanics theory. The numerical method involves subjects such as calculus, partial differential equations and most importantly linear algebra. Specifically for structural-type problems, these methods can then be applied to classic mechanics theories including Hooke's law and D'Alembert's principle [6].

Instead of attempting to solve for an exact solution to the forces and displacements of components with a complicated geometry, elements with finite extent are used to approximate the solution. A displacement is associated with each element and are connected through nodes. Knowing the stress and strain properties of each element, the behavior of neighboring elements and nodes can be found. The complete set of equations describing this behavior results in a set of algebraic equations, which can then

be easily represented in matrix notation and solved simultaneously. Theoretically, the finer the mesh that is used, the more exact a result will be. Although a finer mesh can result in a more accurate solution, the amount of equations increase when the mesh becomes finer, which in turn uses more computational resources. A balance between accuracy and computational resources must be considered to achieve an effective model.

1.2 Literature Review

The use of computational methods as an alternative to empirical testing has grown significantly in the past two decades. A current popular area of research is activity related to the autonomously operated parafoil systems, which are used to accurately deliver cargo to many different chosen locations [7]. Research on the effects of flight characteristics from changes in structural geometry of the canopy in steady flight will allow us to understand how to effectively control the autonomous parachute system.

Previous research has shown the application of structural dynamics simulations, fluid dynamics simulations and coupled Fluid-Structure Interaction (FSI) simulations to tackle the complexity of modeling nonlinear structures like the parachute systems. Proprietary Finite Element (FE) codes have been developed and employed in the past to specifically generate the geometry and flight characteristics of ram-air parachutes in all stages of flight [8]. A limitation to this code is the proprietary nature of the code and its ease of use. Since the code is developed in-house, only the developer understands how to use it, unlike SolidWorks which can be used by anyone trained in similar CAD packages. There have also been successful developments of software that allow different stand alone structural solvers and fluid solvers to be integrated and tackle the ongoing

investigations of FSI problems [9]. There are also certain FSI solvers that combine FE structural simulations with simplified (vortex lattice) fluid solvers [10].

The above mentioned research converges on a similar set of ideas through different approaches. Time, cost, accuracy and ease of use are among the main concepts evaluated through current research. In this work, the effects of a standalone Computational Structural Dynamics (CSD) solver on a full scale ram-air canopy in steady flight using a prescribed pressure distribution is investigated and compared to an in-flight parachute system image. The FE software package LS-DYNA was used for the numerical simulations with the canopy cut-pattern as the starting point. The effects of applied net pressure and pressure distribution as well as the material properties were explored by assessing five different measures of the canopy geometry seen in Section 4.1.

Time and cost can be reduced when making modifications to the cut pattern and overall geometry of a ram-air canopy if a standalone CSD solver can be decoupled from the FSI solution.

Even though numerical simulations have become quite standard for verification and preliminary analysis, it is still not the "be-all and end-all" of parachute design. Lingard [6] provides an in depth analysis on parachute design using empirical data and is the basis of several research endeavors. Empirical testing is still necessary to provide initial data and confirmation of results. Nothing can replace physical testing, but exploring various finite element techniques and refining existing methods as an alternative pushes parachute design a step further in reducing unnecessary allocation of resources during the design cycle.

1.3 Goals

The goals of this project are summarized below:

- Resolve the geometry of a full scale ram-air parachute canopy in steady flight using a combination of commercial solid modeling and finite element softwares including SolidWorks, HyperWorks and LS-DYNA. The software used were chosen due to their compatibility, availability and current implementation in the parachute industry.
- Develop and validate the process required to numerically achieve the inflated ram-air canopy geometry for potential future use.
- Specify parameters for implementation of the process technique which can be applied to variations of the ram-air canopy including different sizes or different cut patterns.
- Explore the effects of various applied pressure amplitudes and distributions on resultant geometry of a specific ram-air canopy.
- Compare the geometry of a full scale parachute canopy in-flight with the simulation results using five defined measurements.

Section 2 discusses the construction of the ram-air parachute model, from a solid geometry with no functional properties to surface membranes, and finally to element membranes. The meshed element model contains functional properties that define the ram-air parachute system such as material properties and boundary conditions. Section 3 introduces a novel approach for developing the geometry of a specific, fully inflated, steady state ram-air parachute system. Section 4 develops and validates the parameters

for an effective simulation model where computational resources reduced without affecting the end results. Section 5 focuses on the effects of modifying simulation model parameters on the geometry of the ram-air canopy. These modified parameters include applied pressure amplitude, applied pressure distribution and suspension line properties.

2. Model Development

In all FE simulations, the main steps include the creation of specific elements, establishing the boundary conditions such as pressure and degrees of freedom (DOF), and applying material properties to the existing elements. More time was spent in this stage of the development than any other stage, which allowed the modification of pressure and material properties to be quick and relatively simple.

2.1 Model Setup

Developing the complete model used in the simulation began with a cut pattern from provided blueprints [4]. This cut pattern consisted of dimensions and angles for each component as well as the overall dimensions for the parachute system. A solid model from this blueprint was created on SolidWorks, an infinitely thin surface membrane model was extracted from the solid using HyperWorks, and finally a mesh with finite elements was created. This was the first of two separate data files used to run the simulation. This could be considered the "skeleton" of the simulation which contained element and node positions.

The second data file contained the functional aspects of the simulation. The information within this file included step size, material properties, loading conditions and constraints. A full sample text is presented in Appendix A.

The two data files could be viewed and modified in text form, and this was beneficial for simple modifications such as pressure or a change in material properties. Using two separate, but interconnected, text files aided in bypassing intermediate pre-processing steps for subsequent simulation runs. This means that system properties could be modified without affecting the meshed geometry and vice versa.

2.1.1 Solid Model

A combination of solid modeling and FE software packages were used to accomplish the goals of the project. A solid model of the MC-4 canopy was created first using SolidWorks CAD software package and the available specifications of the ram-air parachute system. This model had the cut pattern profile for each rib and an undeformed rectangular planform [4]. The solid model was then imported into Altair HyperMesh, the pre/post-processing software, as a parasolid (see Fig.2.1).

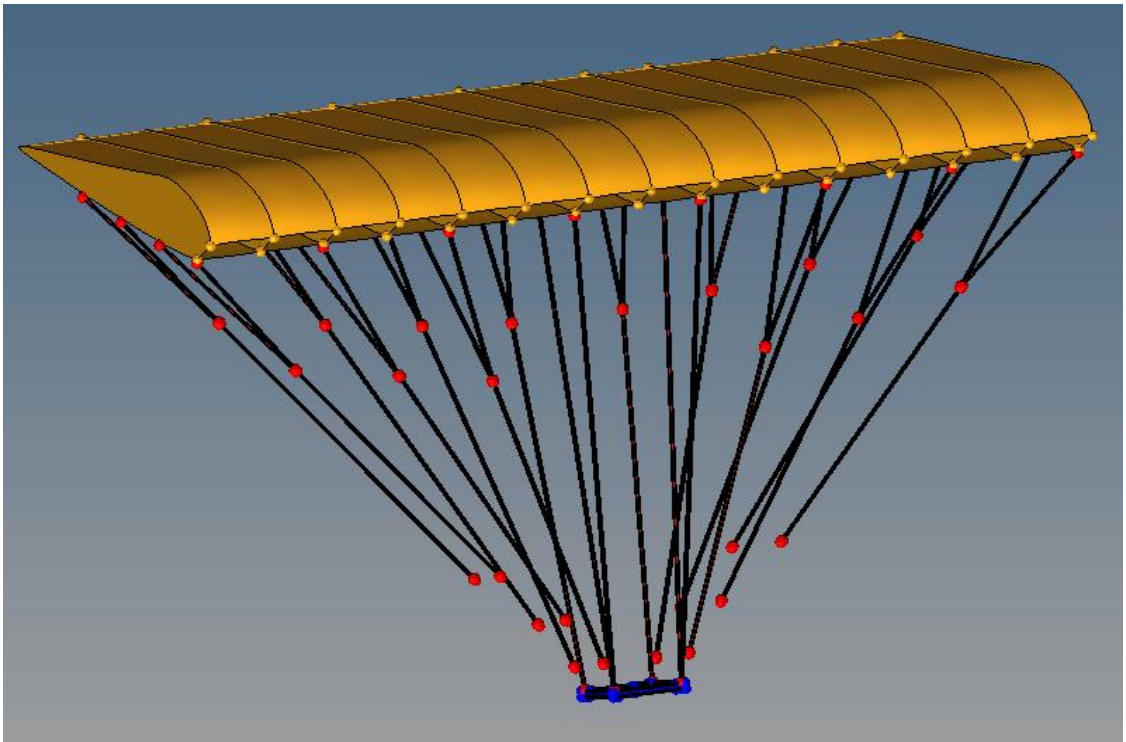


Figure 2.1. Solid model imported from SolidWorks to HyperMesh

It is important to note that the control lines and stabilizers were ignored for the bulk of this project. The stabilizers presented several issues for a clean mesh and were assumed to play a minor role in the inflation and final geometry of the steady flight ram-

air canopy. For any subsequent fluid flow simulations, the stabilizers would make a difference in the results and therefore the stabilizers should be added after the structural geometry of the inflated canopy has been created.

Since the control lines would change length throughout different phases of flight, it was decided that a free floating trailing edge would be observed for the majority of this project. Section 5.2 considers the effects of adding control lines, with a specific line length, to the trailing edge of the ram-air canopy model.

2.1.2 Surface Membrane

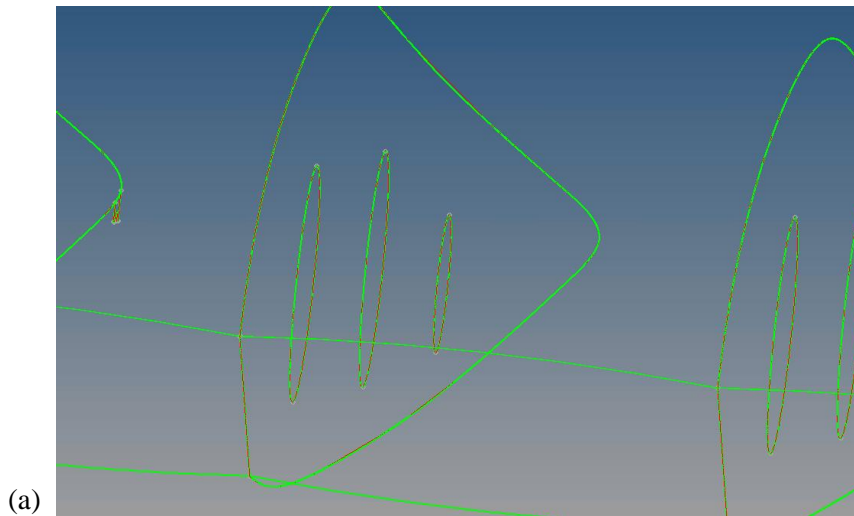
The solid ram-air canopy model was imported into the pre-processing software package, HyperMesh. The surface membranes would be created using appropriate numerical modeling techniques.

The solid geometry was split into sections and grouped into components. For this specific ram-air canopy system, the groups were divided into top and bottom canopy surfaces, left side panel, right side panel, ribs and suspension lines. Partitioning the membranes into specific groups is a common practice in numerical modeling, which essentially takes a complex system and simplifies it for the ease of potential parameter modifications.

Once the groups were created, surface membranes were extracted from the solid geometry. These surfaces were then cleaned in preparation for a smooth and continuous mesh. An in-depth process used to prepare the solid model in HyperMesh for element meshing is outlined in Appendix B.

Planning ahead was a necessary process when constructing this ram-air parachute model. Deciding which components to group would carry on past creating the surface model and into the surface meshing, material application and boundary condition application phases of modeling. This ultimately aided in reducing time during the setup process for subsequent models.

Throughout the "cleaning" phase, the topology mode was activated and can be seen in Fig. 2.2a. Each color represents the status of a particular edge of the model. The red lines represent free edges between two surfaces, the green lines represent a shared edge between two surfaces, and the yellow line represents a shared edge between three surfaces. Figure 2.2b shows the topology of a cleaned model, and can be logically justified. Failure to successfully clean a model led to unwanted gaps, variation in mesh sizes and errors in running the simulation.



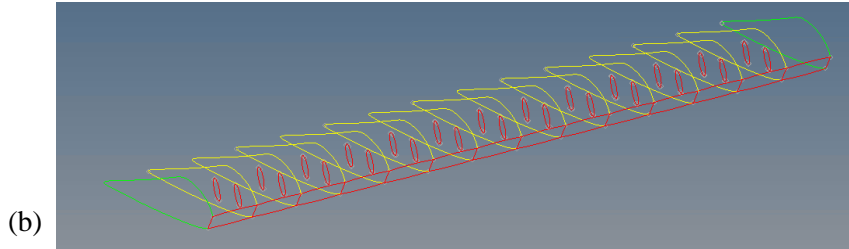


Figure 2.2. Topology of canopy model (a) surfaces prior to cleaning (b) cleaned surfaces

2.1.3 Element Membrane

Once the surfaces were cleaned, a mesh was automatically generated to create a mix of quadrilateral and triangular meshes on the surfaces of each component. Applying a surface deviation of 0.1 in and a minimum element size, depending on the density of the mesh, gave the ability to control certain aspects of the auto generated mesh. The automesh was followed up by the element cleanup command, which was used to identify and clean any failed elements created by an automesh. The default options were used for the element cleanup command. Further minor manual modifications needed to be done to create the smooth and continuous mesh are shown in Fig. 2.3.

The groups created previously simplified the application of an automesh and allowed for isolation of specific components, making the manual mesh refinement less tedious. Properly cleaned surfaces made the difference between 30 minutes of cleaning and several hours of cleaning. The process above can help generate a reliable mesh, in a reasonable time frame, for a very dense mesh that is difficult to clean manually.

Finally, the element types were applied to the existing elements as seen in Fig. 2.3. Seatbelt elements were used to simulate the suspension lines based on their ability to support only tension and not compression. Fabric elements were used for the canopy

surfaces. The final meshed model was then exported as a .key text file and referenced in the LS-DYNA functional data file discussed in Section 2.2 and outlines in Appendix A.

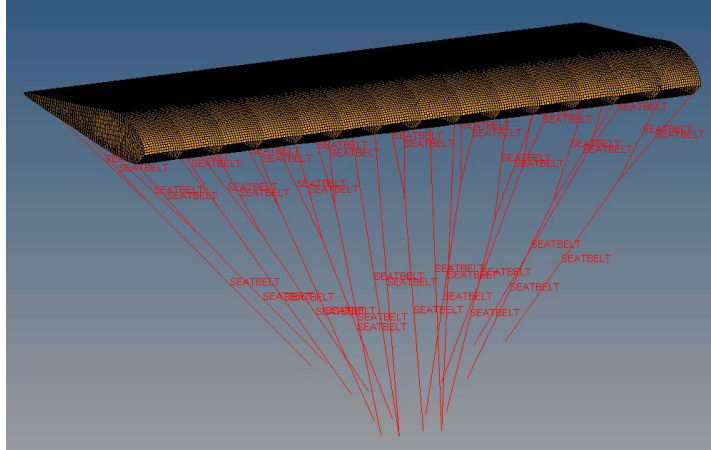


Figure 2.3 Undeformed ram-air canopy with 33037 elements in HyperMesh

2.2 Model Properties

The next step in model preparation was to create a separate text file including the material properties, applied loads, boundary conditions and the control features associated with LS-DYNA.

2.2.1 Material Properties

Since LS-DYNA does not provide the option to display and modify units, it was necessary to specify a set of base units to ensure unit consistency and accurate results. After referencing the LS-DYNA user's manual [11], the units used in this project were $\text{lbf}\cdot\text{s}^2/\text{in}$ (snail or blob) for mass, inches for length, seconds for time, lbf for force and psi for pressure. In this project, pressure was represented by the Pascal unit due to the ease of reference, but psi was used in all simulations.

Material data were extracted from literature which were obtained via empirical testing [12] and specifications such as PIA-C-44378. The material properties are listed in Table 2.1.

Table 2.1. Ram-air parachute model properties [4,12]

Shell (Fabric) Elements			Seatbelt (Suspension) Elements		
Thickness (δ)	0.0028	in	diameter (d)	0.25	in
Mass Density (ρ)	5.0×10^{-5}	snail/in ³	Linear Density	2.9×10^{-3}	snail/in
Young's Modulus (E)	68000	psi	Breaking Strain	30	%
Shear Modulus (G)	7000	psi	Breaking Force	550	lbf
Poisson's Ratio (ν)	0.14	unitless			

The parachute canopy is a type F111 fabric as specified by PIA-C-44378. It is constructed of ripstop nylon, low porosity fabric with 0-3 CFM/ft² permeability [5]. The weave for the ripstop material reduces propagation from small tears and therefore extends the life expectancy of the parachute system.

A thickness of 2.8×10^{-3} in was applied to each shell element representing the ram-air canopy fabric surfaces [12]. This corresponds to the Young's modulus of 6.8×10^4 psi, shear modulus of 7.0×10^3 psi and a Poisson's ratio of 0.14. The mass density was found using PIA-C-44378 Type IV, 1.2 oz/yd² as referenced by the MC-4 canopy specifications [4]. The fabric areal density of 1.2 oz/yd² with a thickness of 2.8×10^{-3} in converts to a mass density of 5.0×10^{-5} snail/in³. This model assumes the fabric material to be isotropic.

$$1.2 \text{ oz/yd}^2 * (1/0.0028) 1/\text{in} * (1/362) \text{yd}^2/\text{in}^2 * 1 [\text{snail}/(\text{lbf} * \text{s}^2/\text{in})] * \\ (1/16) \text{lbf}/\text{oz} * (1/386.4) [(\text{lbf} * \text{s}^2)/(\text{lbf} * \text{in})] = 5 \times 10^{-5} \text{ snail}/\text{in}^3$$

The material property information for the suspension line were limited to a description of braided polyester in the MC-4 canopy specifications. Due to lack of values, a polyester double braided data sheet [14] was used to find the linear density of the suspension lines. The data sheet calls out an approximate weight of 2.4 lbf/100 ft of the double braided polyester lines for a nominal diameter of 0.25 in. Through a similar conversion as the fabric mass density, the result for the linear density of the suspension line was calculated to be 5.176×10^{-6} snail/in. Section 5.3.1 discusses the effects of suspension linear density where ultimately a value of 2.9×10^{-3} was used for all simulations in this project. The breaking strain and breaking force of 30% and 550lbf respectively was given by parachute manufactures. These values can be justified through the same data sheet used to find the linear density [14].

2.2.2 Applied Loads

Given that this project focuses solely on Computational Structural Dynamic (CSD) methods to produce a fully inflated ram-air canopy, a pressure distribution on all surfaces was needed. In previous work [13], the flow around a fully inflated, steady state, ram-air canopy model was computed using a Computational Fluid Dynamic (CFD) solver. A freestream velocity of 12.2 m/s was employed in the CFD simulations. The pressure distribution from the CFD results was used for the current project.

In Section 4 of this paper, a uniform net pressure of 90 Pa, 0.0131 psig, was applied to all interior surfaces of the canopy. This pressure was based off of previous CFD work [13] which found an internal pressure of about 90 Pa. If no previous CFD work existed, the 90 Pa could be also be found by using the dynamic pressure equation of $1/2*\rho*V^2$, with the freestream velocity given by system specifications. There also exists an external suction pressure on the external surfaces of the canopy which would add on to net pressure across the fabric. However, the minimum net pressure of 90 Pa was chosen as the base value.

The process of applying the uniform pressure was simple and straightforward. The top surface, bottom surface and the 2 side panels were selected and grouped into an LS-DYNA card, Set_Segment, which allowed a defined pressure to be applied to the elements associated with those components. The pressure values in the LS-DYNA text file were the only values modified for the pressure case studies in Section 5.1.

Section 5.1 of this paper references and adopts the complete pressure distribution from previous CFD work [13], which consisted of both internal and external pressures. This data was used to calculate net pressure distribution which was applied across the entire surface of the ram-air canopy.

2.2.3 Constraints

The constraints of this simulation ultimately consisted of fixing the end nodes of each suspension line to the four corner nodes of the slider which was fixed in space. Several different variables were considered before arriving to this conclusion, and are discussed in the following sections.

3. Simulation

One of the key goals for this projects was to develop a novel approach to generate a fully inflated, steady state, ram-air canopy using a stand-alone CSD solver such as LS-DYNA. Developing an accurate and robust technique to generate the inflated ram-air canopy geometry using a commercial CSD solver would aid in simplifying preliminary design work in industry and research.

There are currently no readily available techniques to develop the geometry of a ram-air canopy from an initial cut pattern blueprint to its fully inflated steady state. Fluid Structure Interaction (FSI) may be used to achieve this goal, but the complexity of running a coupled CSD solver and a CFD solver has its own set of issues that are still in the process of being developed and refined today.

3.1 Technique Development

The suspension lines, indicated in Fig. 3.1a, were at a pre-defined length. These lines were not fully extended to the slider as they would be in a fully inflated system, and this was one of the largest obstacles in the development of the fully inflated ram-air canopy geometry. The suspension lines towards the spanwise outer edge of the canopy were shorter by design, and the length of these lines were considered to be one of the most important variables in determining the arch, or arc-anhedral, shape of the parachute. The initial approach attempted to artificially extend the suspension lines in order for them to reach the slider while being in its pre-inflated state. Doing this meant that only the suspension lines towards the center of the canopy would have the correct length.

Three different methods were tried to accomplish the goal of resolving a fully inflated canopy, but only one method proved to be robust and effective. The different approaches are briefly outlined below.

The first method consisted of fixing the slider in space and applying a known pressure to the canopy. After each completed simulation, the suspension lines would be trimmed and the process would begin again until the desired line lengths were reached. This method proved to be unrealistic based on how time consuming the pre/post-processing became after each successful simulation in addition to the already existing lengthy run time.

The second method used the same model and concept as the previous, but only the outermost suspension lines were used while all other lines were removed. Once the outer lines were trimmed to the correct length, the inner lines would be reintroduced to the model. Although this method required less iterations and pre/post-processing, it was still too taxing to achieve a proper geometry.

For the third, and most effective method, the idea of trimming the suspension lines was abandoned. Instead, a function of LS-DYNA was used, which prescribed a motion from the end node of the suspension lines to the respective corners on the slider, see Fig. 3.1b. With this technique, the suspension lines were at the correct length and no additional modifications were needed. Only one simulation was required to reach a fully inflated canopy.

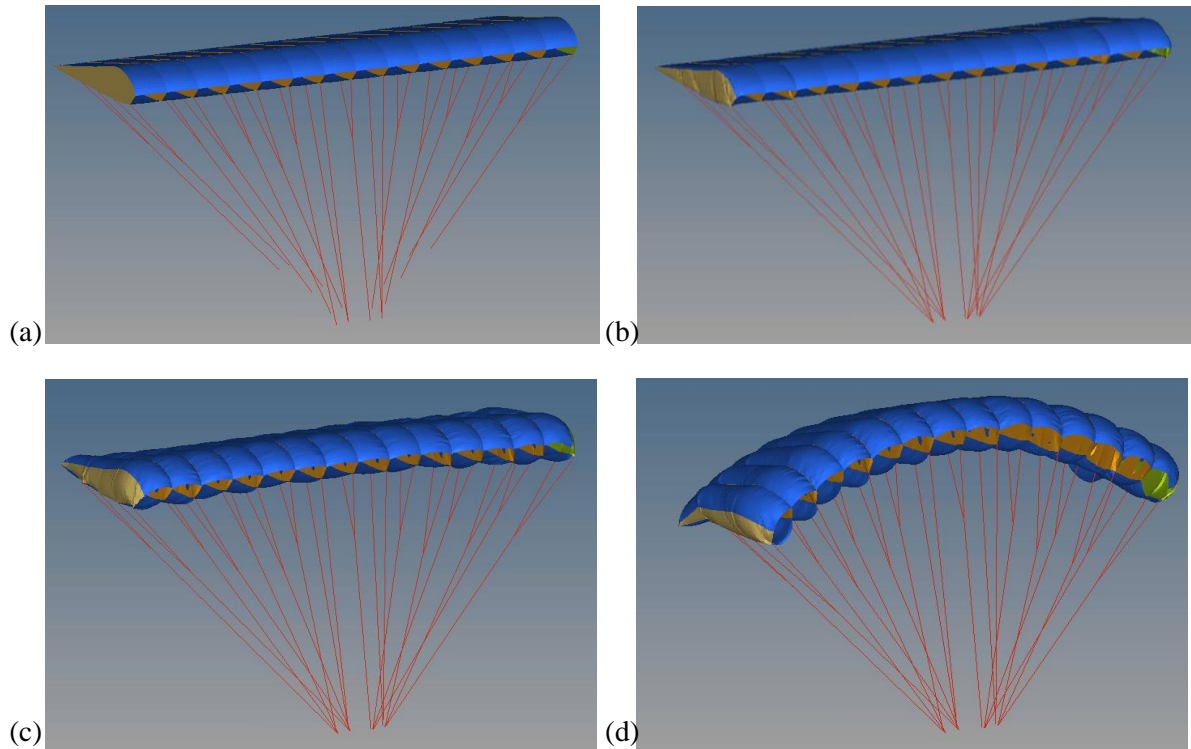


Figure 3.1. Sequence of inflation at (a) $t=0s$, (b) $t=1s$, (c) $t=1.5s$ and (d) $t=25s$ with a uniformly applied net pressure of 90 Pa

From 0.0 s to 1.0 s, the end nodes of the suspension lines were moved from its predefined length to the four fixed corner nodes of the slider. For the remaining time of the simulation, the suspension end nodes were held constant. The applied pressure was not activated until the suspension lines were at their final position on the four fixed corner nodes of the slider. At 1.0 s, the pressure was applied linearly until 1.5 s and then held constant for the remainder of the simulation. This technique and setup was used across the board for all simulations in this project.

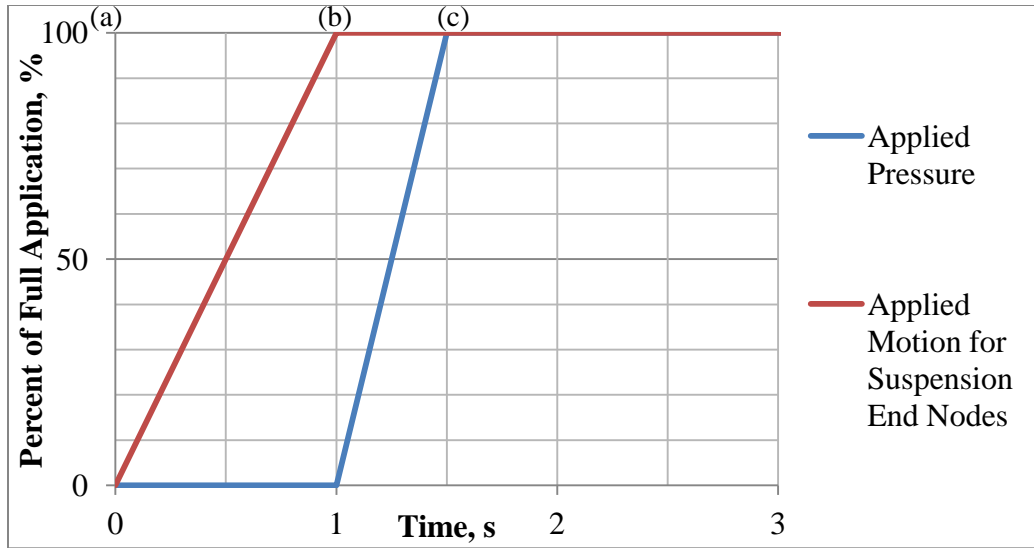


Figure 3.2. Zoomed in view of plot for applied pressure and applied suspension end node motion with time

Figure 3.2 graphically represents the progression of pulling on the suspension lines to the respective corners of the slider and applying a pressure until the geometry has reached a steady state. Figure 3.1 visually demonstrates the same "inflation" sequence.

3.2 LS-DYNA Control Cards

The exact cards and values used to develop Figure 3.1 can be found in Appendix A. Several critical control cards were used to generate the final steady state geometry of the ram-air canopy, and a descriptive list of each card and its function can be seen in Appendix C.

The general function of the cards was to define the model parachute system properties, dictate the simulation run time and generate text files for chosen outputs such as the force in the suspension lines or the displacement of selected nodes. This parachute system could not be accurately modeled without all control cards defined in Appendix A.

4. Canopy Parameters

Before proceeding on to any case studies, certain model parameters needed to be established. The first key consideration was how to identify the final ram-air canopy geometry. A quantitative approach was used, which consisted of selecting measurements that effectively represent the ram-air canopy's in-flight steady state geometry.

The second consideration was the computational run time. Since several simulations were going to be explored, it was imperative to reduce the use of any unnecessary resources. Finding the parachute model's steady state time was considered, therefore reducing the computational run time.

To the same degree, the ram-air parachute model's mesh size effectiveness was also considered. A coarse mesh would consume less computational resources than a more fine and dense mesh. A minimum mesh density needed to be established, which further refinement of the mesh would produce insignificant changes in the five defined measurement's results. Figure 4.1 is a flow chart of the process taken to solve for the steady state time and mesh convergence of the canopy model.

Once the mesh density and steady state time were found, those model characteristics were applied to a series of studies exploring the effects of applied pressure amplitude and distribution. The resulting canopy geometry for the various applied pressure cases were compared.

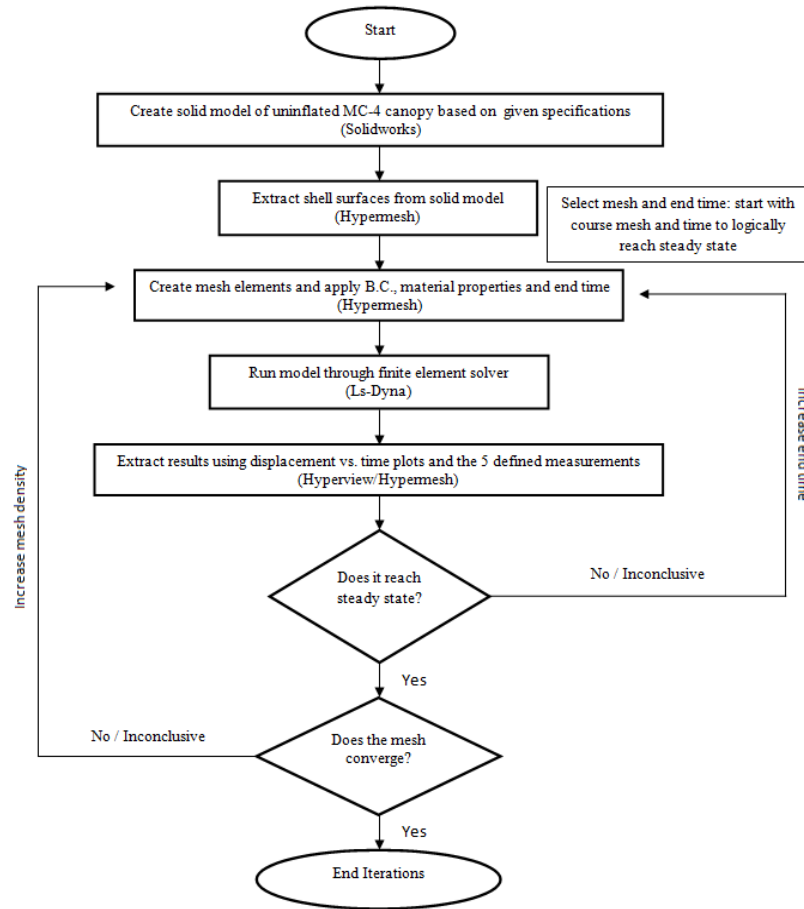


Figure 4.1. Flow chart of the steady state and mesh convergence study

4.1 Defined Measurements

Five different measurements were chosen to represent the overall geometry of the inflated canopy and they are shown graphically in the Fig. 4.2. Each node used for these measurements has a distinct location on the canopy, regardless of mesh size, and can always be identified based on the colors and grouping done in the setup stage of this project. Several common nodes were selected for the five measurements to maintain consistency within the results.

These defined measurements were used to develop and verify the ram-air canopy model's steady state time and mesh effectiveness by comparing the each measured value

as the mesh density was increased. These measurements were also used to compare the extracted values obtained from the full scale canopy in-flight image, Fig. 4.3, to the values generated by the different pressure cases in Section 5.

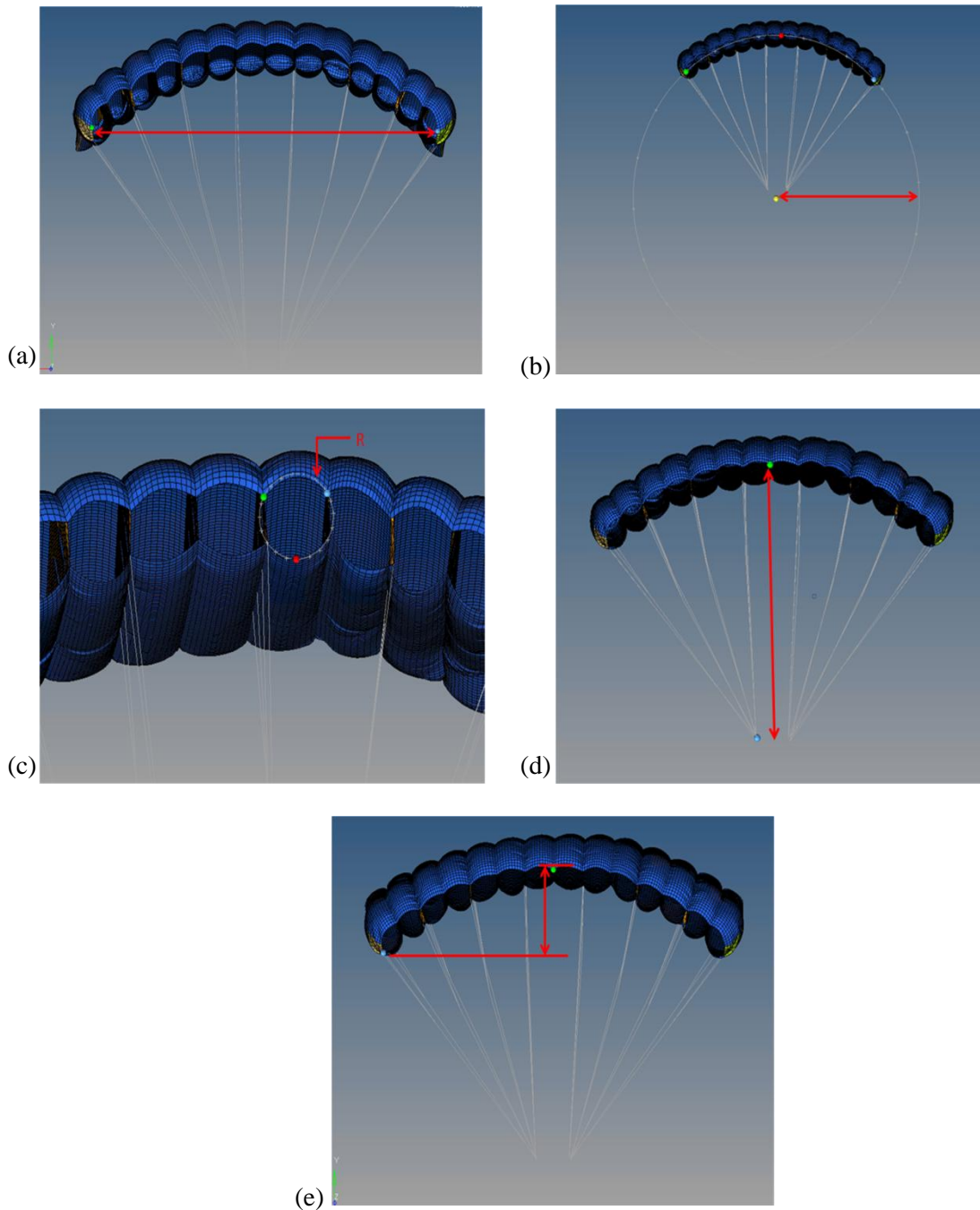


Figure 4.2. Defined measurements (a) M1, (b) M2, (c), M3, (d) M4 and (e) M5

Measurement 1 (M1) was the maximum spanwise extent of the canopy. In the initial uninflated state, the two nodes selected to measure M1 would be located at the outer most corners on the top leading edge of the canopy.

Measurement 2 (M2) was the radius of curvature for the inflated canopy. The same two nodes chosen for M1 were used for M2 in addition to the node at the top surface centerline of the leading edge. The three nodes were then fit to a circle resulting in the radius of curvature.

Measurement 3 (M3) used the same process as M2, where a circle was fitted to each inlet opening. Two of the three nodes were located at the top corners of each half cell, and the third node was located at the bottom center of each half cell. This was done for all 14 openings, then averaged. M3 was used to understand how pressure affected the inlet area

Measurement 4 (M4) was chosen to represent the vertical distance between the slider and the centerline node on the upper leading edge. This showed changes relating to the suspension line properties.

Finally, the fifth measurement (M5) was chosen as the vertical distance between the centerline node on the upper leading edge to the furthest lateral node on the lower leading edge.

An image of a paratrooper in steady descent was available and was imported into SolidWorks. The measurements in Fig. 4.3 were taken at the same locations as the previous five defined measurements. Since the actual length of the slider was 28 in [4], a scale of 1 : 4.9 was calculated and used to extract the five leading edge measurements

from the in-flight image (Table 4.2). A 5% estimated uncertainty was assumed beginning with a rough estimate of the tolerance of the 5.7 slider measurement. ± 0.2 units was selected and divided by 5.7. The result was 3.5%, and the 3.5% was rounded up to 5% based on human error, the slightly skewed image and the resolution of the image. An example for calculating the measurement for the spanwise measurement would be $54.4 * 4.9 = 267$ in.

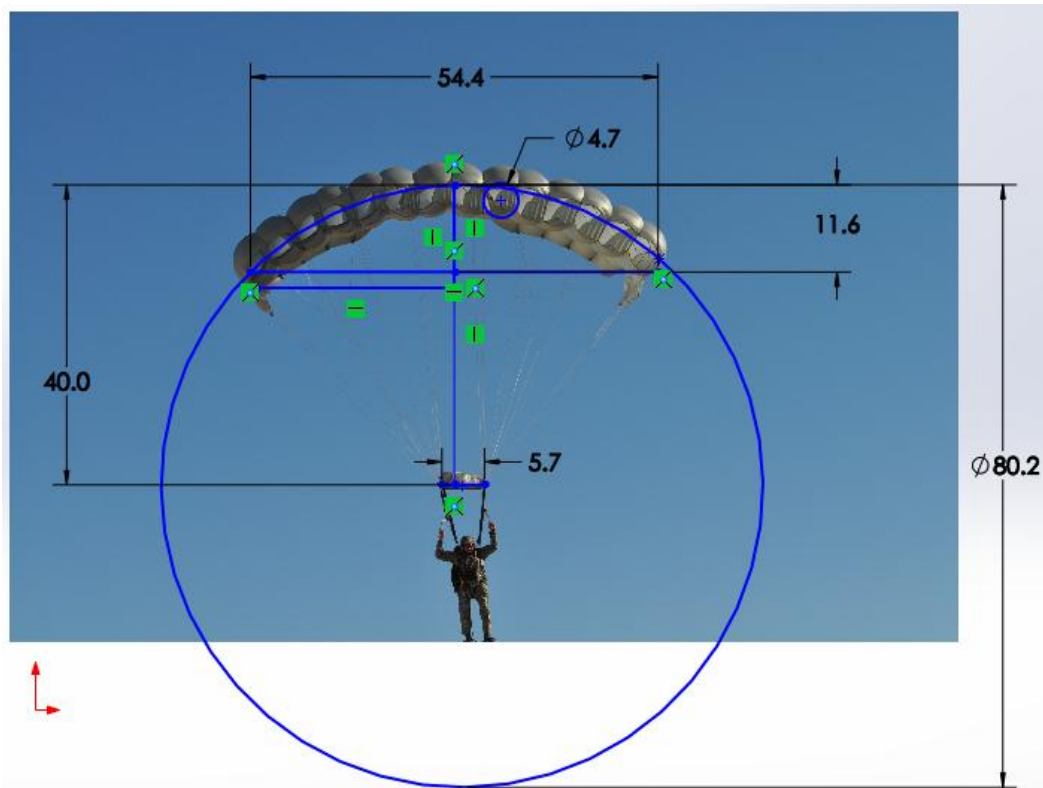


Figure 4.3. In-flight processed image; scale=4.9

4.2 Steady State Time

The properties used to determine the steady state time of the ram-air canopy model were the values provided in Table 2.1 in addition to a uniformly applied net pressure of 90 Pa.

Determining the steady state time was an iterative process. It began with a lightly meshed model containing 3610 elements and had a simulation termination time of 35 seconds. Table 4.1 gives a breakdown of the 5 different sized meshes used in this study.

Three nodes, shown in Fig. 4.4, were used to assess whether the canopy had attained the steady state. The measured nodes spanned the edge of the canopy along the chordwise length and were located at the leading edge (LE), mid-chord edge (MCE) and trailing edge (TE) of the canopy. The latter is where the largest deflection would occur on the canopy. Plots of node displacement versus time showed that the simulation reached steady state after 25 seconds. A 12k element model was then run to verify the steady state time of 25 seconds. The length of time was checked throughout the process of simulating different cases to ensure that making certain modifications to the model would not affect the final steady state.

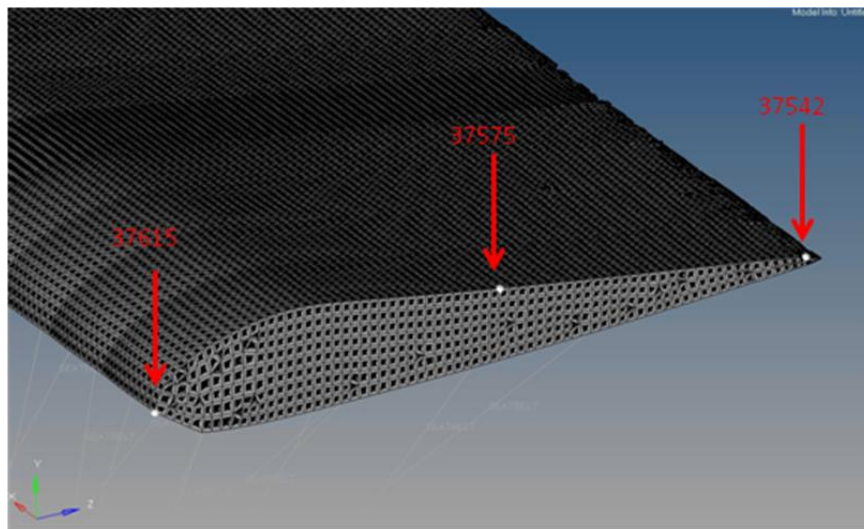


Figure 4.4. Image of N37615(LE). N37575(MCE) and N37542(TE) for the 33k element model

Figure 4.5 shows the vertical displacement of the three nodes with time for the 33k element model. The data show that there is little to no activity after about 25 seconds of run time. The minimum time to reach steady state in this model was one of several factors that helped reduced the size of the file and CPU processing time of subsequent simulations.

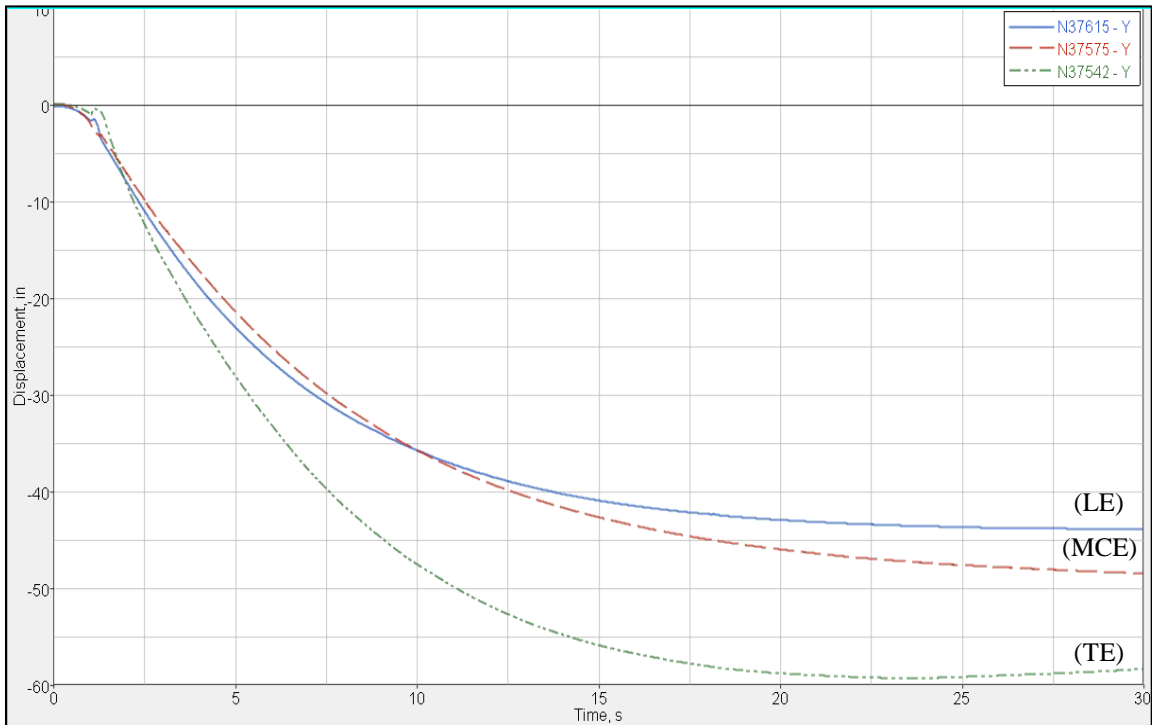


Figure 4.5. Steady state plot of displacement versus time for chosen edge nodes taken from HyperGraph

Further investigation on the data from Fig. 4.5 shows that the base model of this project could be treated as a first order system. The above data was exported into excel where the values were then normalized, plotted and fit to an exponential curve. Figure 4.6 is a sample plot of the leading edge node, N37615.

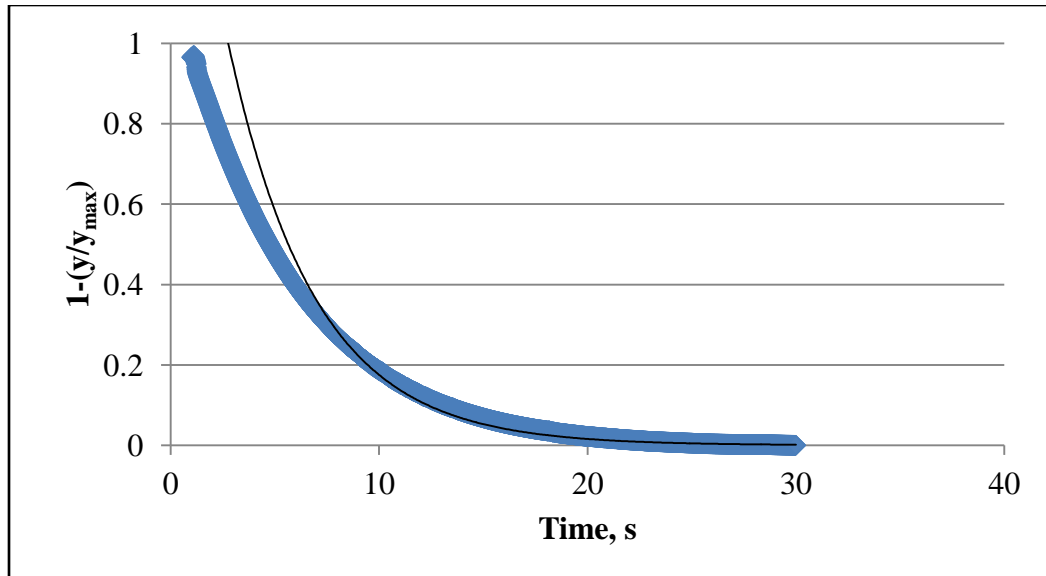


Figure 4.6 Normalized displacement in time for leading edge node

The observed time constant, τ , was similar for the three observed nodes and therefore averaged to $\tau = 4.3$ s. The curve fit equation, $1 - (y/y_{\max}) = 1.95 \cdot e^{-t/\tau}$, characterized the displacement of the canopy in time where y/y_{\max} represented the normalized displacement. Once arranged, the equation became $y/y_{\max} = 1 - 1.95 \cdot e^{-t/\tau}$. A value of 5τ was calculated and resulted in a 99% steady state, hence $5\tau = 21.5$ s for this system. This value verified the time to reach a steady state observed in Fig. 4.5.

4.3 Mesh Convergence

Five mesh sizes were chosen and examined to find the effect of mesh refinement on the defined measured geometry of the MC-4 canopy. Table 4.1 breaks down the number of elements per component of the parachute model. With the exception of the suspension lines, the mesh density of each component was increased from a relatively coarse mesh to a fine mesh until a convergence was reached.

Based on past knowledge and experience with FEA, the initial coarseness of the mesh was estimated in Hypermesh. This mesh needed to contain the largest sized elements possible without sacrificing the cut pattern details of the ram-air canopy model. The process of obtaining a mesh convergence began with a 3610 element model, and continued to increase until the size of the mesh did not affect the results as judged by the five defined measurements discussed in Section 4.1. Each model had a specific number of elements that corresponded to an average area per element listed in Table 4.1. Full canopy values were divided by the area of the canopy resulting in the area per element, i.e. the 3610 element model is equivalent to 39.58 in²/element or an average of 6.3 in x 6.3 in quadrilateral element throughout the model.

Table 4.1. Number of elements for each component of the ram-air canopy model

Model Reference	Full Canopy	Average area per element, in ² /element	Top and Bottom Surface	Left Panel	Right Panel	Ribs	Suspension
4k	3610	39.58	2500	59	54	997	47
12k	12376	11.55	9332	149	144	2751	47
33k	33037	4.33	26254	424	429	5930	47
73k	73107	1.96	59682	893	931	11601	47
100k	100882	1.42	79617	1443	1455	18367	47

Table 4.2 quantitatively shows that the defined measurements begin to reach stable values for the 33k element model. Figure 4.7 graphically verifies this assessment.

Table 4.2 Defined measurements for net pressure amplitude and distribution cases; 33k at
t = 25 s

Model Reference	Elements	Average area. per element, in ² /element	M1, in (x-dist)	M2, in (radius)	M3, in (radius)	M4, in (y-dist)	M5, in (y-dist)
In-Flight Measurements			268.5	198.1	11.6	197.3	57.3
4k	3610	39.58	267.0	202.8	12.4	194.9	58.9
12k	12376	11.55	264.3	198.3	12.6	195.0	57.8
33k	33037	4.33	264.4	201.4	12.1	194.1	56.1
73k	73107	1.96	263.9	199.8	12.2	194.5	56.4
100k	100882	1.42	264.8	200.1	12.1	194.5	56.5

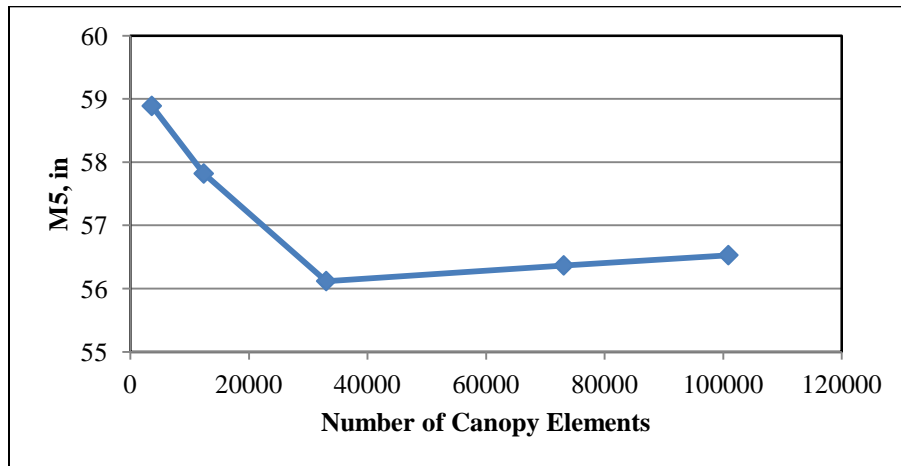


Figure 4.7. Convergence of M5 at the 33k model

The maximum difference between the 4k model and the 33k model occurs for the M5, vertical distance, measurement with a 4.7% change. For that same measurement, M5, the change from the 33k model and the 100k model is 0.73%. The plots from Fig. 4.8 further verify that the measurements for the 33k, 73k and 100k models do not change by more than 1%, and even reached a plateau for some measurements. It is important to note that although the mesh convergence for the following cases was chosen to be 4.33

in²/element (33k), the percent differences across the board does not exceed 5%. The increments on the vertical scale of the plots are no more than 5 inches which is minimal compared to the size of the model. If computational resources are scarce, a mesh with an average area of 39.58 in²/element can be used without sacrificing much accuracy to the geometry, but this may not be a desirable model for CFD analysis purposes. This information is valuable for developing a strategy to design or modify a ram-air parachute system when allocation of resources and accuracy are considered.

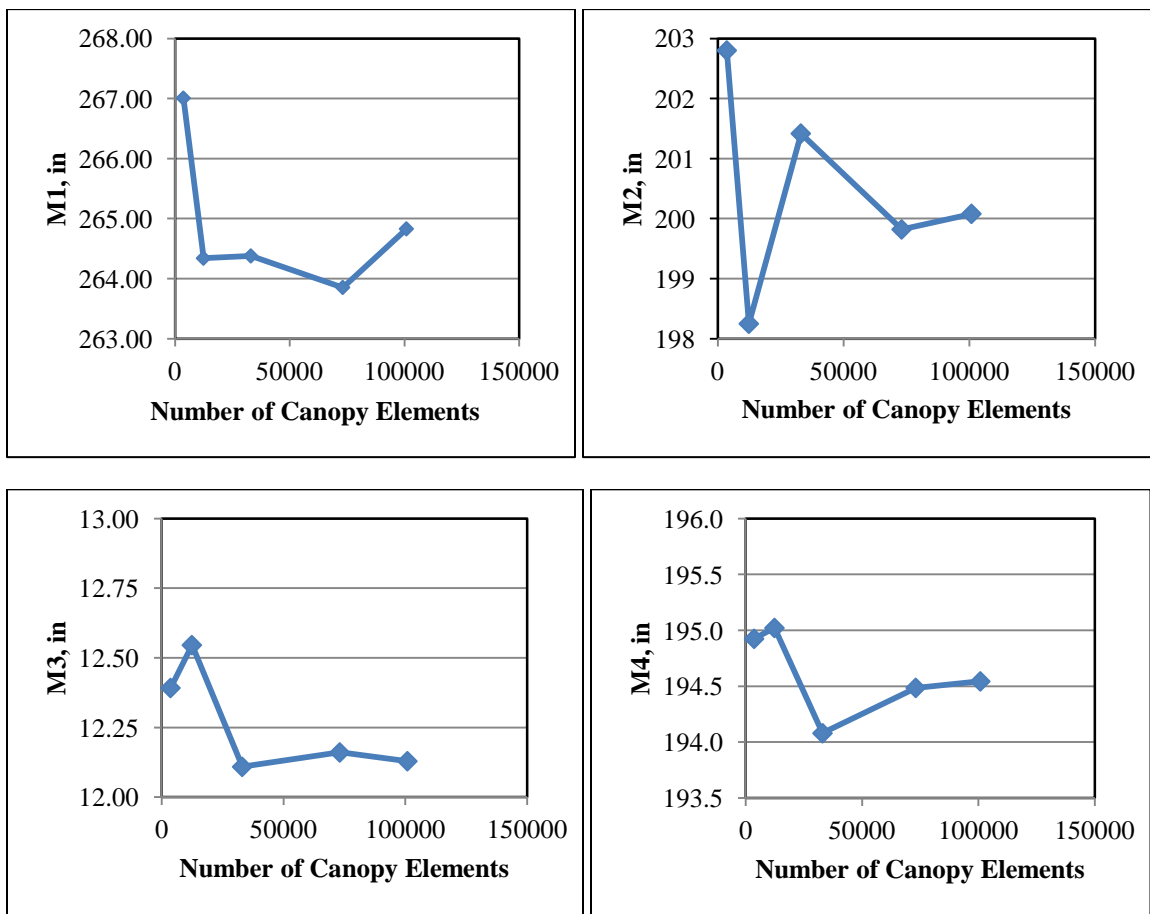


Figure 4.8. Variation of measurements with the number of elements

After finding both the steady state time and minimum mesh density, the results of the 33k model were compared to the in-flight processed image seen in Fig.4.3. The

values given in Table 4.2 result in a maximum of 4.2% change in the leading edge opening radius, M3, and a minimum of 1.6% change in the spanwise extent, M1. These are acceptable results taking into account human error when selecting the points of measurement on the image, and also considering that the in-flight image is not completely square in the frontal view. It can be concluded that increasing the number of elements by a factor of about 27 times the initial 4k model resulted in a maximum difference of about 5% in the defined measurements of the geometry.

5. Results

Several different case studies were constructed and discussed below. They were used to evaluate the capabilities and limitations of utilizing a stand-alone CSD solver to develop a fully inflated, steady state, ram-air canopy geometry.

5.1 Applied Pressure

Three different pressure cases were considered using the 33k element model from Section 4. These cases were constructed to understand the effects of various pressure amplitudes and distribution on the inflated geometry of the canopy. The first case investigated the effects of uniform net pressure in a range of 45 Pa to 270 Pa in increments of 45 Pa. Recall that a net pressure of 90 Pa was the baseline value.

The second case, variable pressure in the chordwise direction (VPC), applied a piecewise average pressure across the top, bottom and side surfaces of the canopy. The top and bottom surfaces of the canopy were separated into 6 different sections as shown in Fig. 5.1. This pressure profile was then applied uniformly in the spanwise direction for the top and bottom surfaces. The side panels were assigned an overall average pressure of 140 Pa.

The third case, variable pressure in the chordwise and spanwise direction (VPCS), used the same concept of slicing the pressure into multiple sections across the spanwise as well as the chordwise directions. Each variable pressure case involved extracting the pressure profile data from the previously run CFD model [13].

5.1.1 Uniformly Applied Pressure

Since a base model was already constructed in the previous sections, applying multiple uniform net pressures across the surface was a straightforward task. The 33k model was used with just a modification to the applied net pressure values in the text files. Six uniformly applied net pressure values were implemented, and the leading edge measurement were recorded and listed in Table 5.1.

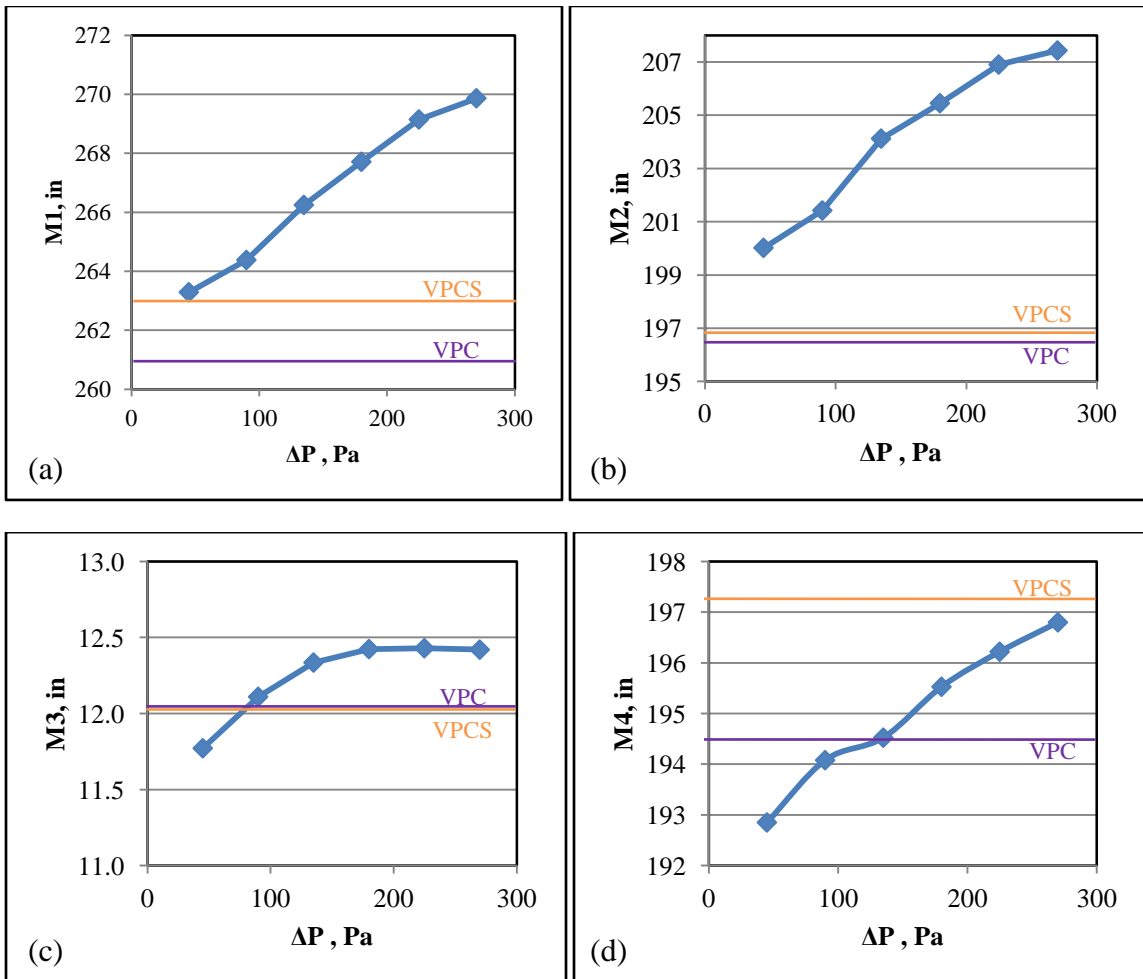
Table 5.1. Measurements taken for uniform pressure and variable pressure cases with the 33k model and $t = 25s$

Pressure, Pa	M1, in (x-dist)	M2, in (radius)	M3, in (radius)	M4, in (y-dist)	M5, in (y-dist)
In-Flight	268.5	198.1	11.6	197.3	57.3
45	263.3	200.0	11.8	192.9	55.2
90	264.4	201.4	12.1	194.0	56.1
135	266.3	204.1	12.3	194.5	56.2
180	267.8	205.5	12.4	195.5	56.5
225	269.2	206.9	12.4	196.2	56.9
270	269.9	207.4	12.4	196.8	57.1
VPC	260.8	196.5	12.1	194.5	53.4
VPCS	263.0	196.9	12.0	197.3	56.2

The measured results for uniform net pressure show a slight linear increase in each of the five measurements as the uniform net pressure increases. The plots from Fig. 5.1 compare the data for the uniform net pressures as well as the pressure distribution cases, variable pressure in the chordwise direction (VPC) and variable pressure in the chordwise and spanwise directions (VPCS).

The relationship between deflection and net pressures are qualitatively comparable since a heavier load in a physical air drop will stretch the suspension lines as pressure gets increased, Fig. 5.1d, and will also try to flatten out the canopy as expressed with an increase in M1 and M2 (Fig. 5.1a-b). M3 shows that the billowing for the leading

edge opening of the canopy increases by 5.5% from 45 pa to 180 Pa and then reaches a plateau of about 12.4 in as shown in Fig. 5.1c. The overall maximum change for the uniformly applied pressure case was 5.5% for M3 and a minimum change of 2.1% for M4. These variations can be considered small when compared to an applied net pressure increase of 6 times from the lowest applied pressure of 45 Pa. In general, the simulations were able to capture many of the steady state behavior of the parachute using a uniformly applied net pressure model. It also showed that the fully inflated, steady state, ram-air canopy geometry was not sensitive in the chosen range of uniformly applied net pressures.



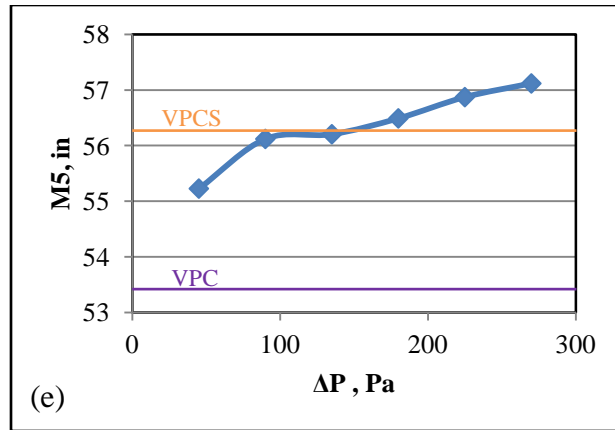


Figure 5.1. Variation of the 5 measurements with the applied pressures

5.1.2 Variable Pressure in the Chordwise Direction (VPC)

The pressure profile data for the VPC model was extracted from the CFD simulations [13] where the centerline of each half-cell was observed for all 14 half cells. The canopy was chosen to have an angle of attack of 10° and a freestream velocity of 12.2 m/s, resulting in a dynamic pressure of 90 Pa.

This data was extracted as the pressure profile along the internal and external surfaces in the chordwise direction of the ram-air canopy. The difference between the internal and external pressures resulted in a net pressure distribution, see Fig. 5.2. The calculated net pressure was equal to the difference between the inner and outer surface pressures.

Once the net pressure profile plots were created, the surface was partitioned into six regions, and the net pressure values for each region were averaged. For example, region 1 results in a maximum net pressure of 210 Pa and a minimum net pressure of 190 Pa, therefore the value used in the model was 200 Pa.

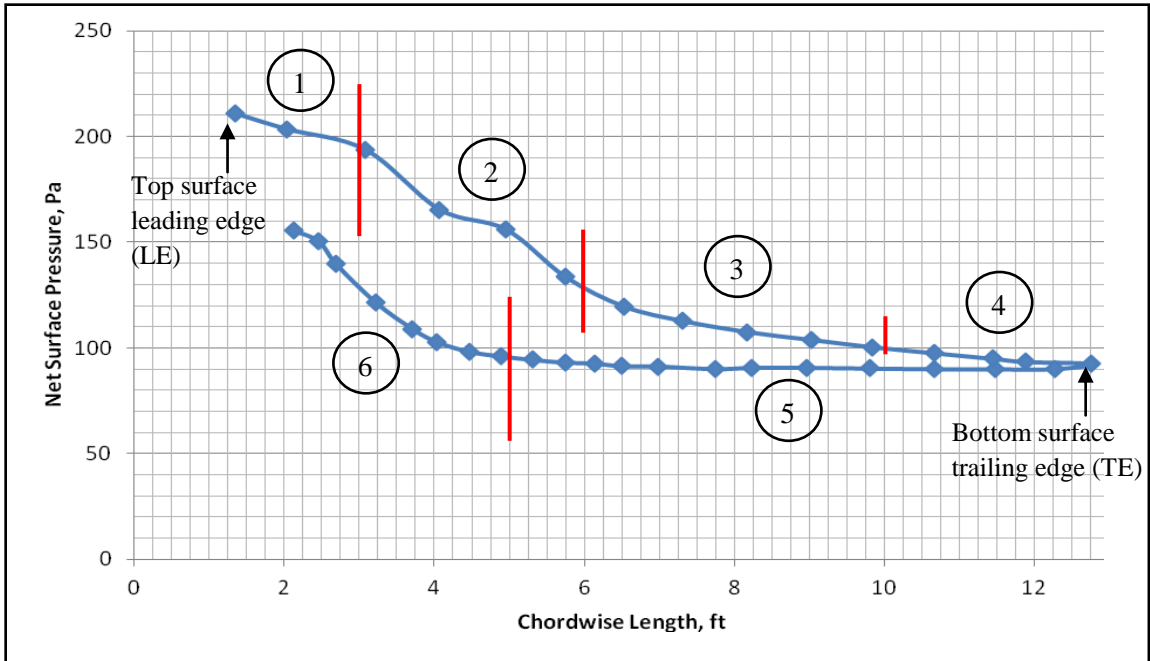
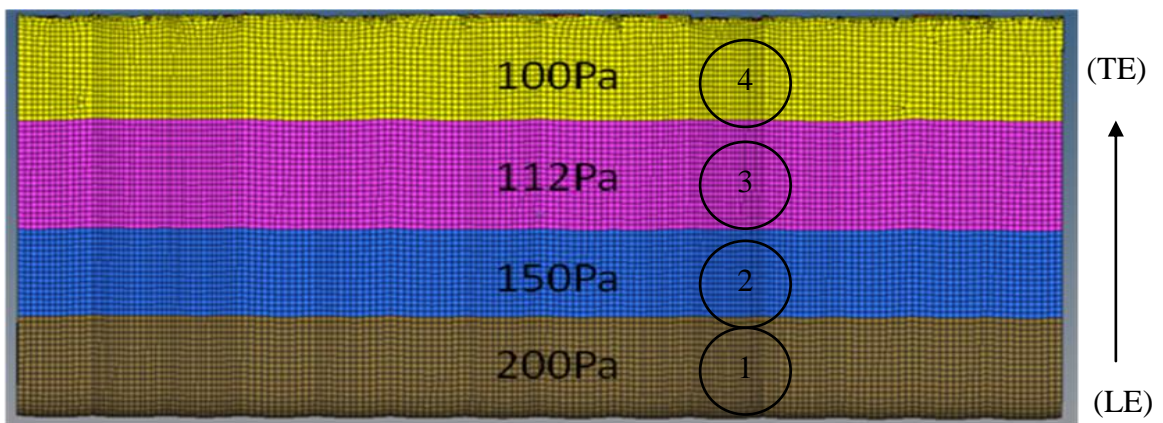


Figure 5.2. Plot of net pressure for the middle half cell extracted from CFD data

In order to apply this distribution to the FE model, the net pressure distribution was divided into four regions on the upper surface and two regions on the lower surface. These six regions are shown in Fig. 5.3; the upper surface regions extend to 3 ft, 6 ft and 10 ft from the leading edge where as the lower surface was split at 5 ft from the leading edge. For the VPC case, only the center half cell's pressure data were used.



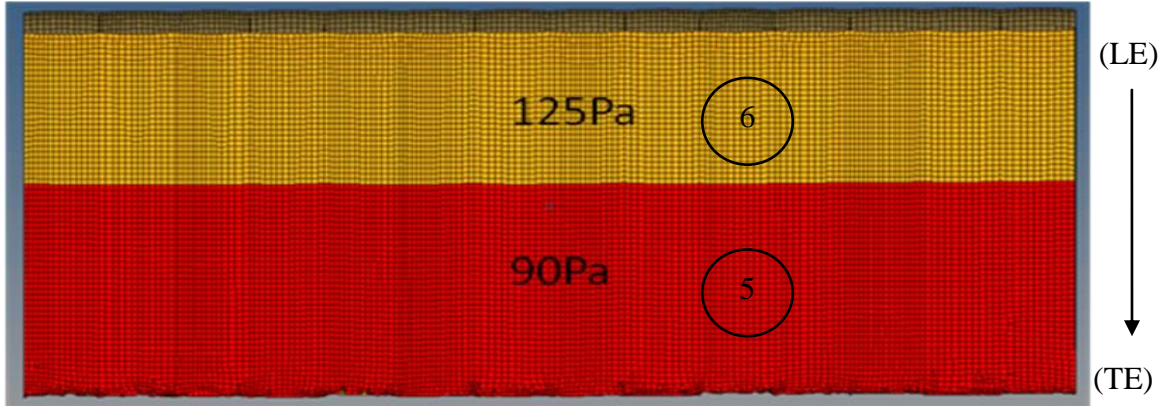


Figure 5.3. Applied net pressure for VPC on the (a) top surface and (b) bottom surface

The measurements taken from the VPC model were used to compare to the base model with a uniformly applied 90 Pa pressure. The maximum difference between the two model results was 4.9% in the vertical deflection, M5, and a minimum of 0.17% in the cell opening, M3. The more accurate applied pressure model, VPC, results did not vary by much in comparison to the base model results. This information may be significant for preliminary design work in industry.

5.1.3 Variable Pressure in the Chordwise and Spanwise Direction (VPCS)

The process of constructing the VPCS case followed the same steps as the VPC case in Section 5.1.2. The primary difference between the two cases was that the VPC case only used one half cell net pressure data while the VPCS case used the net pressure data for all 14 half cells, Fig. 5.4. Note that a net pressure of over 200 Pa exists on the top of the canopy even though the stagnation pressure on the interior of the canopy is only 90 Pa. This was due to the suction pressure on the exterior surface of the canopy.

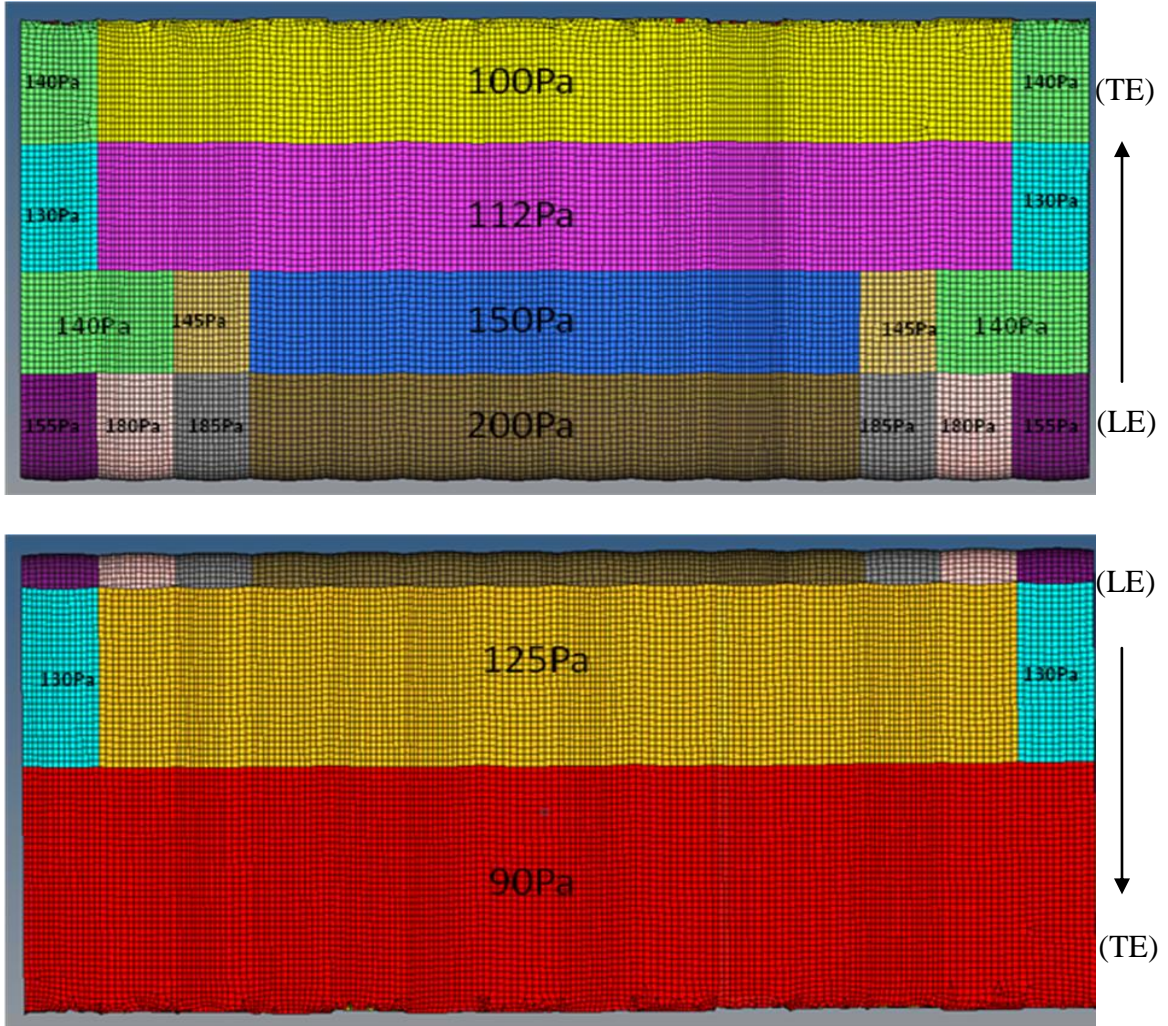


Figure 5.4. Applied net pressure for VPCS on the (a) top surface and (b) bottom surface

The third and final applied pressure case should represent closest pressure distribution to a steady state ram-air parachute in flight. Comparing the VPCS case to the 90 Pa base model resulted in a maximum difference of 2.3% in the radius of curvature measurement, M2. When compared to the in-flight image measurements, a maximum difference of 3.6% in M3 was recorded. It is now solidified that applying various types of pressure amplitudes and distribution on the CSD simulation, using the technique described in Section 4, will not affect the final geometry significantly.

5.2 Implementing Control Lines

After observing the images in Fig. 5.5, it became apparent that the free floating trailing edge deflection varied with the applied net pressure. This observation revealed the need to reintroduce the control lines to the simulations.

5.2.1 Trailing Edge Measurements

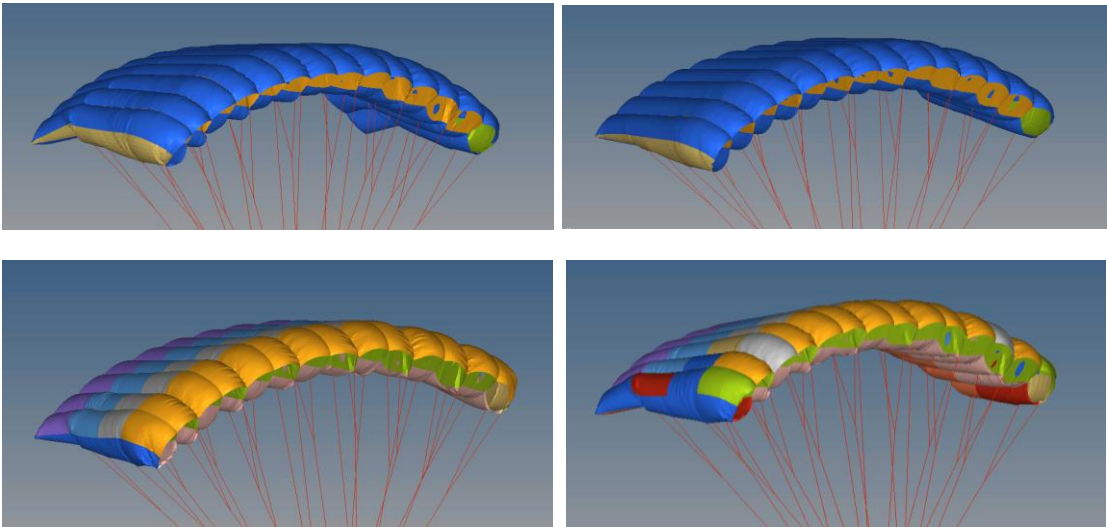


Figure 5.5. Steady state canopy for uniform (a) 90Pa, (b) 270Pa, (c) VPC and (d) VPCS

Differences in the canopy geometry between the uniform applied pressure and variable applied pressure cases cannot be clearly identified visually in Fig. 5.5, except one significant difference at the trailing edge deflections. Since the 90 Pa and VPCS case had very similar trailing edge behavior, and the maximum change in the leading edge measurements was 2.4% in M2, the possibility of using the uniformly applied 90 Pa model as an alternative to the VPCS case was investigated. The process of applying a uniformly applied pressure to a simulation would consume less resources compared to the

VPCS case. Three additional measurements were chosen to further understand the effects of various applied pressures on the trailing edge of the canopy.

Figure 5.6 shows the node points of measurement at the centerline of the span length (N26250), the outer most point in the span length (N44582) and a location in between (N32724).

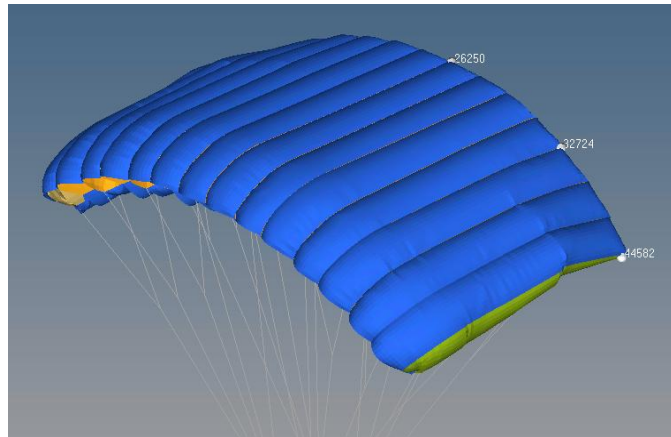


Figure 5.6. Image of 3 measured nodes at the trailing edge of the canopy

For the uniform pressure case, the trailing edge begins to reach a point of equilibrium as the pressure increases. Figure 5.7c shows that the trailing edge of the canopy begins to plateau at 180 Pa for the corner node. The remaining nodes from Fig. 5.7a-b continue to slightly increase then decrease as the pressure increases. Comparing the VPC and VPCS cases to the uniform pressure case presents a significant difference with a maximum difference of 47.6%, from -11.4 in to -6 in, for the centerline node (N26250) and a minimum difference of 11.8%, from -65.1 in to -57.4 in, for the outer node (N44582). Without the control lines on the trailing edge, it is unclear whether or not

the uniformly applied, 90 Pa, model can be chosen as an alternative for the complete VPCS model.

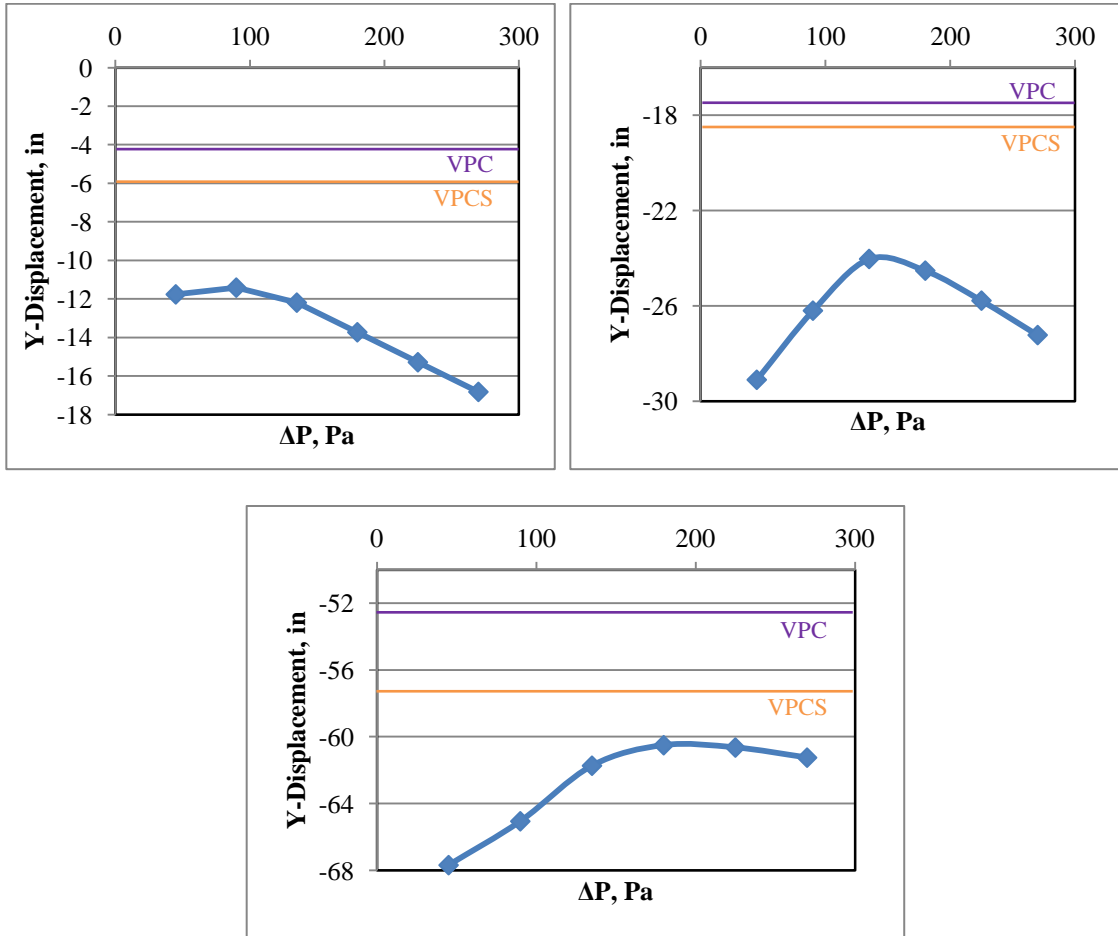


Figure 5.7. Plot of trailing edge nodes (a) N26250, (b) N32724 and (c) N44582 with the applied pressure

5.2.2 Control Lines

Since the length of the control lines may vary throughout flight, a specific length was chosen and implemented to verify the use of the uniformly applied, 90 Pa, model as an alternative to the VPCS model. Figure 5.8 shows the addition of control lines to the trailing edge of the canopy at 80% of its fully extended state on the uninflated cut pattern.

Measurements were taken for the 90 Pa and VPCS inflated models and showed a maximum of 15.9% change, from -12.2 in to -10.3 in, for N26250 and a minimum of 2.8% change, from -39.9 in to 38.7 in, for N44582. The five defined measurements, M1 - M5, were similar to the previous study comparison of the 90 Pa and the VPCS models which did not exceed 2.3%. Considering the 15.9% change in height is 2 in, it is clear that the uniformly applied, 90 pa, model can be used as an alternative for the VPCS case.

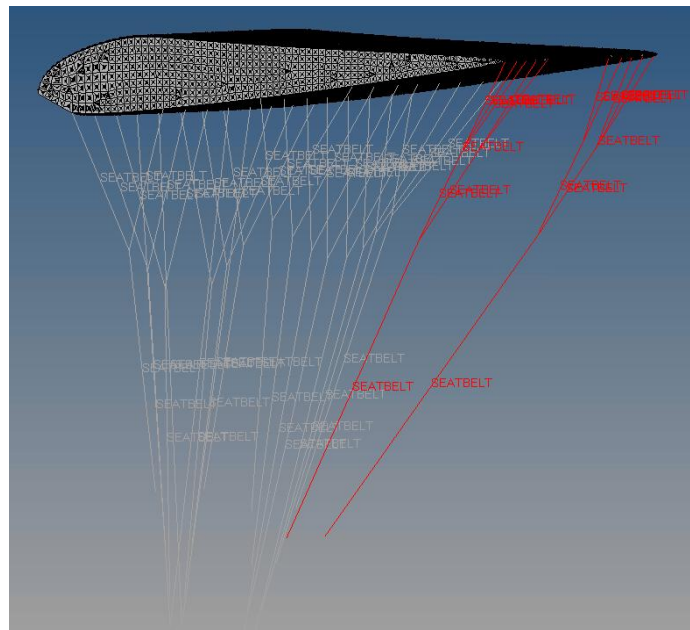


Figure 5.8. Image of added control lines at 80% full extension

5.3 Suspension Line Linear Density

Initial attempts to inflate the canopy in Section 3 resulted in issues of stability of the parachute system as seen in Fig. 5.9. As the uniform pressure was being applied to the surface of the canopy, the entire system began to pitch backwards. It was concluded that the combination of applying a uniform pressure and the cut pattern's declining slope of the canopy in the chordwise direction created a resultant net force in the flow direction.

Further simulation testing showed a direct correlation of the parachute system's instability in the simulation to the suspension line linear density of 5.176×10^{-6} snail/in.

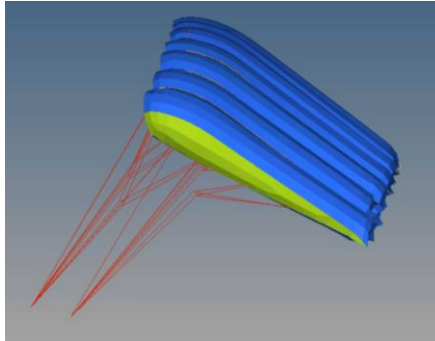


Figure 5.9. Unstable parachute system

In order to constrain the unwanted pitching of the canopy, three equally spaced nodes were fixed in the x-y plane (Fig. 5.10). Although sufficient data was obtained, more issues surfaced with this technique. Each model contained a localized deformation in the location of the fixed nodes. In CFD simulations, small irregularities on the surface can affect the results¹³. For this project, it was very important to allow the canopy to naturally inflate, wrinkle and crease, but adding fixed nodes did not allow this.

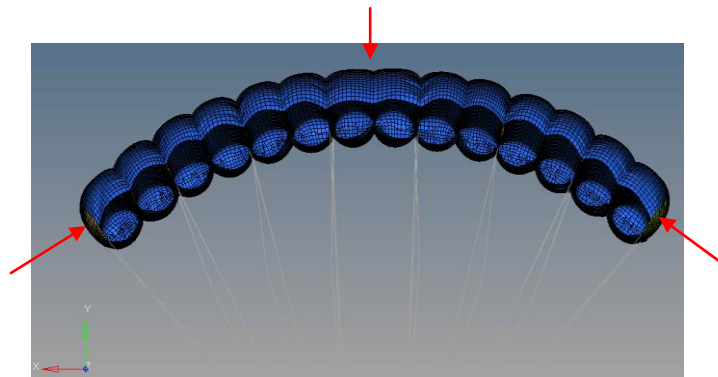


Figure 5.10. Inflation after applying fixed nodes to the top leading edge of the canopy

In addition to the localized deformation, the inability to reach a steady state in the trailing edge of the canopy was an issue. More boundary conditions would need to be applied to the model in order to result in a steady state measurement for the trailing edge. To avoid complicating the simulation any further, the linear density of the suspension lines were increased to the point that the resulting drag-type force in the canopy would not cause the parachute system to pitch backwards. Increasing the linear density, and essentially the mass, created stiffer suspension line elements. It was assumed that, for FEA simulation, the more dense the suspension lines were, the more simulation time it would take for the drag-type force to move the system in the flow direction. This was a critical concept which added to the uniqueness of the developed technique for this project.

Since the length of the suspension lines dictate the arc-anhedral shape of the canopy, it was expected that the results of the 5 defined leading edge measurements for a model with a more dense suspension line would be similar to the smaller, 5.176×10^{-6} snail/in density measurements.

Results were recorded after increasing the linear density of the suspension lines to 2.9×10^{-3} snail/in while keeping the percent elongation and breaking force unchanged. These results reaffirmed the assumption that the geometry would not vary significantly. Once the linear density of the suspension lines were increased, the canopy was able to inflate naturally without any fixed nodes on the surface of the ram-air canopy. The entire canopy reached a steady state, and the maximum difference in the results of the smaller linear density model compared to the higher linear density model was 3.4% in M5 at the 33k model. Figure 5.11 shows that the trend for the M5 displacement was maintained, but

the curve was shifted down. This meant that the 1000 times heavier suspension line restricts the deflection by only 3.4%. A portion of this difference can also be attributed to the local deformation caused by fixing the nodes on the canopy surface.

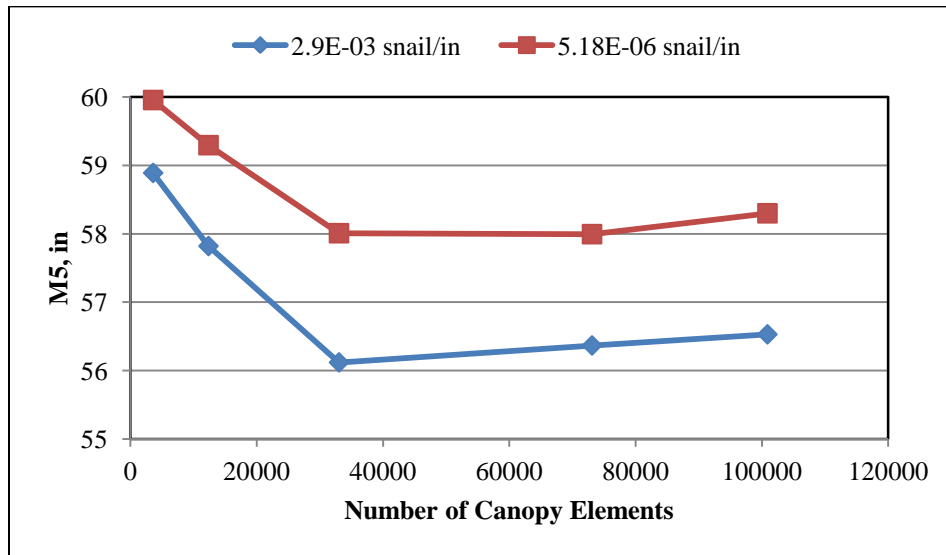


Figure 5.11. Plot of suspension linear densities for M5

The main difference between the two approaches was the time to reach a fully inflated, steady state, model. The actual linear density of 5.18×10^{-6} snail/in took 2 seconds to reach a steady state and required nodes to be fixed on the surface of the canopy. The larger, 2.9×10^{-3} snail/in linear density, took 25 seconds to reach a steady state but did not require any fixed nodes on the surface of the canopy. Further analysis showed that the desirable value for the suspension's linear density is 1.0×10^{-3} snail/in, which reduces the steady state time by half and does not require additional boundary conditions to successfully inflate the ram-air canopy (Table 5.2).

Table 5.2. Linear density and steady state time relationship

Linear Density [snail/in]	Time to steady state [s]	Does canopy need to be fixed in x-y plane?
5.18E-06	2	Yes
6.00E-04	6	Yes
1.00E-03	12	No
2.90E-03	25	No

Figure 5.12 shows that there was a linear relationship between the time to reach steady state and the linear density of the suspension line.

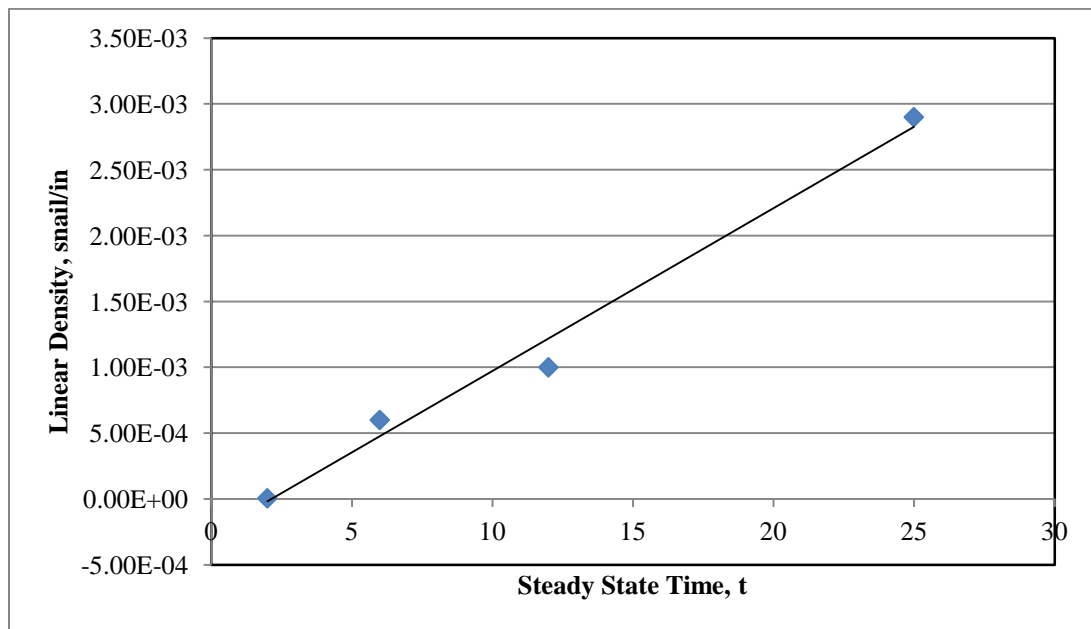


Figure 5.12. Suspension line linear density as a function of steady state time with a best fit line equation of $y = 0.0001x - 0.0003$

5.4 Vented Models

The information gained from this project was applied to three unique, vented, ram-air parachute models. These models utilized the material properties from Table 2.1 as well as a uniformly applied pressure of 90 Pa. Figure 5.14 shows all three models

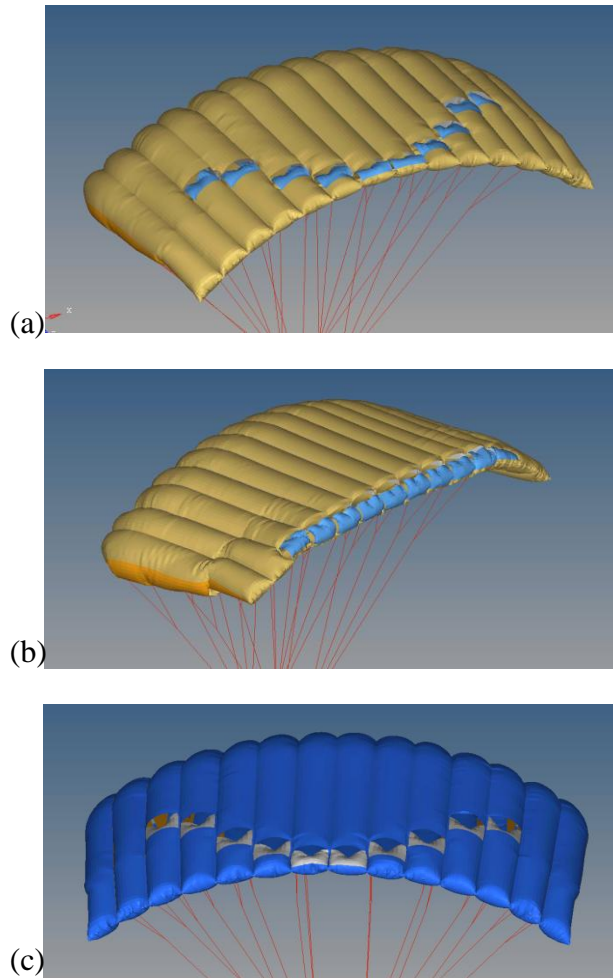


Figure 5.13 Vented cases with (a) rectangular openings in a V-pattern (b) rectangular openings in-line and (c) triangular openings in a V-pattern

The parameters and techniques found within this paper produced the fully inflated, steady state, geometry seen in Fig. 5.13, and these results are visually similar to models without the vents. This showed a lot of promise by being able to generate a steady

state canopy model for a modified cut pattern using a stand-alone CSD solver. General behavior of the canopy in steady state could be captured without the use of complex FSI simulations. Further work, including exporting the geometry and preparing a solid model for CFD purposes, will be carried out to simulate the flow around this canopy.

6. Conclusion

The value of this work comes from the established normalized model parameters, the results of the applied pressure study and the technique used to achieve the geometry of a ram-air canopy in steady flight using commercial solid modeling and finite element software packages.

Ultimately, a mesh with an average area of $4.33 \text{ in}^2/\text{element}$ was chosen which can be used to determine a minimum mesh density for various sized ram-air canopies. The mesh calculated should aid in reducing computational resources and creating a smooth surface without compromising accuracy. It was also discovered that the time it takes for the ram-air canopy to reach a steady state is highly dependent on the linear density of the suspension lines. A linear line density of $1.00 \times 10^{-3} \text{ snail/in}$ was chosen with a steady state time of 12s to be the most efficient value using the method of prescribing a motion to the suspension lines.

In regards to pressure, it was found that applying a stagnation pressure of 90 Pa uniformly across the surface of the canopy creates a percent change in geometry of about 2% compared to a model with a variable pressure accurately depicting the profile across both the chord and span length. Depending on the priorities of the user, the time to generate a model with variable pressure may not justify the 2% difference.

In the larger picture of modeling the geometry of a steady state ram-air canopy, it can be concluded that the application of various types of pressure will not greatly affect the end result. The most critical variables in modeling the geometry is the length of the suspension lines and the material properties of the model.

Lastly, a relatively accurate geometry for a canopy in steady flight can be generated without the use of a FSI solver. This can be useful in an industry setting for preliminary design work.

References

1. Jalbert, Domina C. "Multi-cell wing type aerial device." U.S. Patent No. 3,285,546. 15 Nov. 1966.
2. Desabrais, Kenneth J. and Johari, Hamid, "Experimental Investigation of Parachute Canopies with Rectangular Parallelepiped Geometries," *Journal of Aircraft*, Vol. 50, No. 1, pp. 197-203, 2013.
3. Lingard, J. Stephen, "Ram-Air Parachute Design," *13th AIAA Aerodynamic Decelerator Systems Technology Conference and Seminar*, AIAA, Clearwater Beach, May, 1995, pp. 10-23.
4. U.S. Army Natick research, Development and engineering center, "MC-4 manufacturing plans," 1990-1991.
5. Headquarters, Department of the Army, "Unit and direct support maintenance manual for MC-4 Ram-air free-fall personal parachute system," NSN 1670-01-306-2100, July 2003. Also available from URL retrieved October 2014:
<http://www.liberatedmanuals.com/TM-10-1670-287-23-and-P.pdf>
6. Logan, Daryl L., *A First Course in the Finite Element Method*, 5th ed., Stamford, Connecticut, 2012, pp.2-27.
7. Altmann, Dr.-Ing. Horst, "Numerical Simulation of Parafoil Aerodynamics and Dynamic Behavior," *20th AIAA Aerodynamic Decelerator Systems Technology Conference and Seminar*, AIAA, Seattle, WA, May, 2009.
8. Zhu, Yan, Moreau, Melissa, Accorsi, Michael, Leonard, John, Smith, John, "Computer Simulation of Parafoil Dynamics," *16th AIAA Aerodynamic Decelerator Systems Technology Conference and Seminar*, AIAA, Boston, MA, May, 2001.
9. Charles, Richard D., "Application of Airdrop Systems Modeling Software," *19th AIAA Aerodynamic Decelerator Systems Technology Conference and Seminar*, AIAA, Williamsburg, VA, May, 2007.
10. Chatzikonstantinou, T., "Problems in Ram Air Wing Modeling and their Solution in the Three Dimensional Simulation Code "PARA3D"," Proceedings of the 15th CEAS/AIAA Aerodynamic Decelerator Systems Technology Conference, Toulouse, France, June 1999, AIAA paper 99-1716.
11. Livermore Software Technology Corporation. (2012). LS-DYNA. *User's Manual*. Livermore, California. LSTC
12. Niemi, Eugene E. Jr., "An Improved Scaling Law For Determining Stiffness of Flat, Circular Canopies," Technical Report Natick/TR-92/012, 1992.

13. Eslambolchi, Ali, "Computation of Flow Over a Full Scale Ram-Air Parachute Canopy," Master's Thesis, Mechanical Engineering Dept., Cal State University, Northridge, Northridge, CA, 2012.

14. "Polyester Double Braid." Cortland. Web. 10 Mar. 2014.
<http://www.cortlandcompany.com/sites/default/files/downloads/media/product-data-sheets-polyester-double-braid_1.pdf>.

Appendix A: Sample file for 33k model

```

1 *KEYWORD
2 *INCLUDE
3 Basic_Canopy_11.key
4 $
5 $-----1-----2-----3-----4-----5-----6-----7-----8
6 $
7 *CONTROL_TERMINATION
8 $$  ENDTIM  ENDCYC  DTMIN  ENDENG  ENDMAS
9     25.00
10 $
11 *CONTROL_TIMESTEP
12 $$  DIINIT  TSSFAC  ISDO  TSLIMIT  DI2MS  LCTM  ERODE  MSIST
13     0.0     0.9     0     0.0     0.0     0     0     0
14 *CONTROL_DYNAMIC_RELAXATION
15 $$  NRCYCK  DRTOL  DRFCTR  DRTERM  TSSFDR  IRELAL  EDTTL  IDRFLG
16     100     5E-3  0.995  0.05  0.9     0     0.0  -999
17 $
18 $
19 $-----1-----2-----3-----4-----5-----6-----7-----8
20 $
21 *DATABASE_GLSTAT
22     0.020
23 $
24 *DATABASE_MATSUM
25     0.020
26 $
27 *DATABASE_SBTOUT
28     0.020     3
29 $
30 *DATABASE_NODFOR
31     0.020     3
32 $
33 *DATABASE_SPCFORC
34     0.020     3
35 $
36 *DATABASE_NODAL_FORCE_GROUP
37     21
38 $
39 *SET_NODE
40     21
41     7601
42     7602
43     7603
44     7604
45     37615
46     26327
47     16232
48     7555
49     7554
50     7546

```

```

51      7560
52      7559
53      7550
54      7600
55      7599
56      7598
57      7597
58      7596
59      7595
60      $
61      $
62      *DATABASE_BINARY_D3PLOT
63      $ DT/CYCL      LCDT      NOBEAM
64      | 0.010
65      $
66      $-----1-----2-----3-----4-----5-----6-----7-----8
67      $
68      $
69      *MAT_FABRIC
70      $HMNAME MATS      2Canopy
71      $      MID      RO      EA      EB      EC      PRBA      PRCA      PRCB
72      | 2 5.0000E-5 68000.0 00000.0 0.0000000 0.1400000 0.0000000
73      $      GAB      GBC      GCA      CSE      EL      PRL      LRATIO      DAMP
74      | 7000.0 0.0000000 0.0000000 1.0 100.000 .05 0.15
75      $      AOPT      FLC      FAC      ELA      LNRC      FORM
76      | 0.0000000
77      $      A1      A2      A3
78      | 0.0000000 0.0000000 0.0000000 0.0000000 0.0000000 0.0000000
79      $      V1      V2      V3      D1      D2      D3      BETA
80      | 0.0000000 0.0000000 0.0000000 0.0000000 0.0000000 0.0000000
81      $
82      *MAT_SEATBELT
83      $HMNAME MATS      3Suspension
84      | 1 .00239 21 21
85      $
86      $
87      *DEFINE_CURVE
88      | 21 0.0000000 0.0000000 0.0000000 0.0000000
89      | 0.0000000E+00 0.0000000E+00
90      | 0.3000000E+00 550.000E+00
91      $
92      $-----1-----2-----3-----4-----5-----6-----7-----8
93      $
94      *PART
95      $HWCOLOR COMPS      3      49
96      Canopy
97      | 1 2 2
98      $HWCOLOR COMPS      3      49
99      Side1
100     | 2 2 2

```

```

101 $HWCOLOR COMPS      3      49
102 Side2
103      3      2      2
104 $HWCOLOR COMPS      3      49
105 MidSection
106      4      2      2
107 $HWCOLOR COMPS      2      57
108 Suspension
109      5      1      1
110 $
111 $-----1-----2-----3-----4-----5-----6-----7-----8
112 $
113 *SECTION_SHELL
114 $HMNAME PROPS      2Canopy
115      2
116      .003      .003      .003      .003
117 *SECTION_SEATBELT
118 $HMNAME PROPS      3Suspension
119      1
120 $
121 $-----1-----2-----3-----4-----5-----6-----7-----8
122 $
123 $ CONTACT CARDS WHEN NEEDED
124 $
125 $-----1-----2-----3-----4-----5-----6-----7-----8
126 $
127 $
128 *BOUNDARY_PRESCRIBED_MOTION_NODE
129 $HMNAME LOADCOLS      1auto1
130 $HWCOLOR LOADCOLS      1      11
131      7555      1      2      102      -2.798
132      7555      2      2      102      -8.394
133      7555      3      2      102      -2.601
134      7554      1      2      102      -14.58
135      7554      2      2      102      -24.074
136      7554      3      2      102      -6.977
137      7546      1      2      102      -36.991
138      7546      2      2      102      -42.153
139      7546      3      2      102      -11.617
140      7560      1      2      102      -3.589
141      7560      2      2      102      -10.325
142      7560      3      2      102      -1.092
143      7559      1      2      102      -17.091
144      7559      2      2      102      -27.156
145      7559      3      2      102      -2.745
146      7550      1      2      102      -41.522
147      7550      2      2      102      -45.578
148      7550      3      2      102      -4.398
149      7600      1      2      102      2.755
150      7600      2      2      102      -8.243

```

```

151      7600      3      2      102      -2.504
152      7599      1      2      102       14.58
153      7599      2      2      102     -24.074
154      7599      3      2      102     -6.977
155      7598      1      2      102     36.991
156      7598      2      2      102    -42.153
157      7598      3      2      102    -11.617
158      7597      1      2      102     3.589
159      7597      2      2      102    -10.325
160      7597      3      2      102     -1.092
161      7596      1      2      102     17.091
162      7596      2      2      102    -27.156
163      7596      3      2      102     -2.745
164      7595      1      2      102     41.522
165      7595      2      2      102    -45.578
166      7595      3      2      102     -4.398
167      7601      1      2      102     0.000
168      7601      2      2      102     0.000
169      7601      3      2      102     0.000
170      7602      1      2      102     0.000
171      7602      2      2      102     0.000
172      7602      3      2      102     0.000
173      7603      1      2      102     0.000
174      7603      2      2      102     0.000
175      7603      3      2      102     0.000
176      7604      1      2      102     0.000
177      7604      2      2      102     0.000
178      7604      3      2      102     0.000
179      *LOAD_SEGMENT_SET
180      $95Pa Applied Pressure
181      | 1      101 -0.013779
182      $
183      $
184      $-----1-----2-----3-----4-----5-----6-----7-----8
185      *DAMPING_GLOBAL
186      | 4      1.0      1.0      1.0      1.0      1.0      1.0
187      $
188      *DEFINE_CURVE
189      $
190      | 4      1.0      1.0
191      |      0.0      200.0
192      |      1.0      200.0
193      |      25.0      200.0
194      $
195      *DEFINE_CURVE
196      $
197      | 101      1.0      1.0
198      |      0.0      0.0
199      |      1.0      0.0
200      |      1.5      1.0
201      |      25.0      1.0
202      *DEFINE_CURVE
203      $
204      | 102      1.0      1.0
205      |      0.0      0.0
206      |      1.0      1.0
207      |      25.0      1.0
208      $
209      $-----1-----2-----3-----4-----5-----6-----7-----8
210      $
211      *END

```

Appendix B: Canopy Model Pre-Processing Procedure

The following procedure is used to create a meshed model from a solid model.

1. Split the geometry into sections and group into components. For this project, the canopy was grouped into top/bottom canopy surface, left side panel, right side panel, ribs and suspension.
2. Use the midsurfacing (under geometry->surface edit) tool to create surfaces from solid geometry.
3. Isolate the canopy components including the ribs and side panels.
4. Extend (under geometry->surface edit) the surfaces to fill gaps and connect free edges.
5. Manually edit lingering edges and points to establish a fully cleaned surface.
6. Isolate suspension lines and create nodes at the points of intersection as well as the four corners on the slider.
7. Create 1D elements from the nodes created in the previous step

Appendix C: LS-DYNA Control Cards

Below lists the most important LS-DYNA control cards used in this project. Each card contributed important features to simulate real inflation as accurately as possible.

- **Contol_Termination** - Controls the end simulation time, but differs from CPU processing time of the simulation.
- **Control_Timestep** - Constantly calculates the largest possible stable time step size to reduce solution time while maintaining accuracy.
- **Control_Dynamic_Relaxation** - Initializes stresses and deformation to simulate a preload. Once the preloaded state is achieved, the time resets to zero
- **Mat_Fabric (Type 34)** - Used for quadrilateral and triangular membrane elements undergoing large deformations. Originally developed for airbag materials.
- **Mat_Seatbelt (Type B01)** - Material only supports tension, and produces zero force when slack occurs.
- **Section_Shell** - Defines node locations and thickness for each fabric element.
- **Section_Seatbelt** - Defines node locations for each seatbelt element.
- **Boundary_Prescribed_Motion_Node** - Defines the 3D displacement of suspension line end nodes to the respective corner of the slider.
- **Load_Segment_Set** - Used to apply pressure onto fabric elements.
- **Damping_Global** - Dampens the displacements caused by applying pressure and assisted in stabilizing the parachute system.
- **Define_Curve** - Used on above cards to control the limits of each function.